



UiT The Arctic University of Norway

Department of Arctic and Marine Biology

Parasite Communities in Arctic Blue Mussels - Exploring Spatial and Temporal Dynamics

Femke E. de Ruiter

Master's thesis in Biology BIO-3950, August 2024



Abstract

Blue mussels (*Mytilus* spp.) play an important role in intertidal ecosystems along coastlines worldwide. Trematodes, which often parasitize these mollusks, can effectively alter blue mussels' functional role in intertidal ecosystems. Due to the trematodes complicated life cycles and manifold but hidden effects on the intertidal ecosystems, they are often ignored in marine research, especially in understudied areas. This study explores the community dynamics of trematodes within Arctic Norwegian blue mussels on various spatial and temporal scales. In the Sommarøy area, differences in trematode infection intensity and infection prevalence between human-influenced and natural sampling locations, between wave-exposed and sheltered sampling sites, and differences along the intertidal gradient and seasonal dynamics were tested. In a sample of 1557 blue mussels, three trematode species were identified (*Renicola* sp., *Gymnophallus* sp., and *Himasthla* sp.), of which *Renicola* sp. and *Gymnophallus* sp. occurred frequently. The abundance of *Renicola* sp. was negatively affected by human influence, wave exposure, and an increase in intertidal level, while no such trends were observed for *Gymnophallus* sp. Further, it was observed that *Renicola* sp. increased slightly in infection intensity in the later phase of the vegetative period (fall) in Arctic intertidal zones. This thesis takes a multidimensional approach to unravel antagonistic, interactive, and additive effects on the infection dynamics of trematodes within blue mussels and provides a baseline to understand these organisms and their implications in Arctic ecosystems.

Table of Contents

| | |
|---|----|
| 1. Introduction | 1 |
| 2. Material and Methods..... | 7 |
| 2.1 Site Description | 7 |
| 2.2 Sampling..... | 9 |
| 2.2.1 Mussel Sampling | 9 |
| 2.2.2 Additional Biodiversity Assessments..... | 9 |
| 2.3 Mussel Dissection and Parasite Identification | 9 |
| 2.4 Statistical Analysis of Trematode Data | 10 |
| 2.4.1 Infection Intensity | 10 |
| 2.4.2 Prevalence | 12 |
| 2.5 Additional Biodiversity Data Processing | 12 |
| 3. Results | 14 |
| 3.1. Trematode Infections..... | 14 |
| 3.1.1 Infection Intensity | 15 |
| 3.1.2 Prevalence Analyzed as Infection Likelihood..... | 21 |
| 3.2. Additional Biodiversity Data | 26 |
| 4. Discussion | 28 |
| 5. References | 37 |
| 6. Appendix | 47 |

Foreword

This thesis is the final product of my studies here at UiT and would not have been possible without the support and guidance of many people and my fellow students by creating a great learning environment that made me enjoy coming to university.

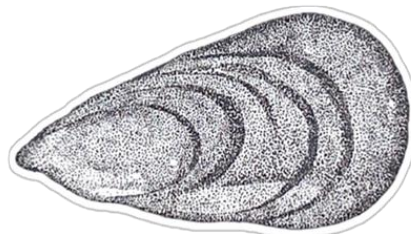
First of all, I want to thank the freshwater group here at UiT.

I want to thank Marcus Molis and Victoria for inspiring me in the choice of my sample locations and measuring intertidal levels at the sampling sites.

Many people supported and accompanied me during my fieldwork, including Eleni, Juan, my Dad, Josephine, Bas, and Robin. Special thanks to Josephine and Nicole for helping me out during the fall sampling. Also, thank you to Johanna and Karin for helping me with the equipment. Nigel and Gabrielle, your additional support was very appreciated when I struggled with the statistics.

Thank you, **Ana Born-Torrijos**, for accompanying me during my project and answering my emails and questions.

I also want to thank my main supervisor **Christian Selbach**, for his guidance, patience, and support throughout this project.



1. Introduction

Norway's coastal ecosystems are of great importance, as they hold diverse habitats spread across the world's second-longest coastline, ranging from 58° to 71°N, reaching above the Arctic circle (Haarpaintner & Davids, 2021). Extreme climatic conditions including great disparities in light availability and temperature between summer and winter define especially the northern parts of this area. Additionally, accelerated global warming in the Arctic, or “polar amplification”, where temperatures increased 2 to 4°C during the last 50 years, makes these coastal ecosystems distinctive habitats and important areas for research for global change (Walsh, 2008).

Along coastlines, blue mussels (*Mytilus edulis*, *M. galloprovincialis*, and *M. trossulus*) are a common sight and play an important role of biological, cultural, and monetary value (Brooks & Farnen, 2013; Gosling, 2008; Wilson et al., 2013). Dense colonies of mytilids, known as mussel banks, can, for example, increase heterogeneity in intertidal zones and create habitat for other species such as barnacles (*Semibalanus balanoides*) or algae (e.g. *Chondrus crispus*). Moreover, these mussel banks can filter-feed on runoff or eutrophic water in coastal zones, increasing water clarity and mitigating human pollution (Bracken et al., 2012; Eggermont et al., 2020; Gosling, 2008; Jones et al., 1994). Blue mussels thus contribute to the modification, maintenance, and creation of coastal intertidal zones and are therefore considered ecosystem engineers (Eggermont et al., 2020; Gosling, 2008; Jones et al., 1994).

In the intertidal zone, blue mussels are exposed to pressures and stressors of terrestrial systems at low tide in addition to aquatic ones during high tide and have adapted to these extreme environments (Lauckner, 1983; Nagarajan et al., 2006). In addition to these abiotic stressors, biotic stressors, such as predators as well as parasites and pathogens require further morphological, physiological, and behavioral adaptations to increase mussel survival (e.g. Benito et al., 2023; Bouallegui, 2019; Nagarajan et al., 2006). Predation by vertebrate predators such as various fish species, gulls, and anseriform birds, which rely on blue mussels as a food source, can have a bottom-up effect on intertidal food webs (Horn et al., 2017; Liénart et al., 2021). Mussels therefore connect pelagic, intertidal, and coastal ecosystems (Horn et al., 2017; Bracken et al., 2012; Hilgerloh, 1997).

As blue mussels play an important role in connecting aquatic and terrestrial ecosystems, parasites associated with blue mussels can rely on this connectivity to complete their complex life cycles (i.e. Bracken et al., 2012; Marcogliese & Cone, 1997). Often, metazoan parasite taxa,

such as helminths, pass through a parasitic larval stage within blue mussels as one of their intermediate hosts, before developing into a sexually mature adult parasite in their vertebrate final hosts (Wright, 1960). While relying on their hosts, parasites impose costs and possibly impair their hosts' overall fitness, at least partially. Examples of parasite-induced costs in mytilids range from reduced filtration abilities, impaired shell formation, to reduce ability of production of byssal threads for attachment (Khosravi et al., 2023; Lauckner, 1983; Lauckner, 1984; Mouritsen et al., 2022; Stier et al., 2015).

These effects demonstrate that even though the individual body mass of each parasite is small, their effect on ecosystems can be great when considering their ecological interactions (Morley, 2012). Parasite-host relationships can therefore be understood as analogous to predator-prey relationships and should be acknowledged as such in ecosystem studies, as both interactions can provoke direct lethal and sub-lethal effects and trigger defensive responses and thus can cascade through whole ecosystems (Raffel et al., 2010; Thieltges et al., 2024). Such effects can be even greater when parasites infect central ecosystem engineers, such as blue mussels, which regulate important ecological processes (Mouritsen et al., 2022).

Contrary to well-studied predator-prey relationships, however, the ecological implications of parasite-host relationships beyond obvious disease effects have long remained overlooked to characterize and explain ecosystems (Buck, 2019; Lafferty et al., 2008). To fully understand the ecological interactions and food web dynamics, it is crucial to include the effects parasite communities can have on the ecosystems they are part of, as they change ecosystem interactions and influence the survival and behavior of their hosts (Lafferty et al., 2008; Marcogliese, 2004; Marcogliese & Cone, 1997; Mouritsen et al., 2022). In the last decades, the roles of parasites in food webs, community structure, and trophic cascades have increasingly been included in ecological assessments, not only by looking at direct density and trait-mediate impacts (e.g. reduced fitness) of parasites on their hosts but also at indirect density and trait-mediated effects on hosts and their environment (Buck, 2019; Dunne, 2013; Lafferty et al., 2008; Sukhdeo, 2010; Thieltges et al., 2024, Werner & Peacor, 2003).

Trematodes are one of the most common parasites found in blue mussels (Buck et al., 2005). These digenean flatworms have species-specific, complex life cycles, with at least one invertebrate first intermediate host (usually a mollusk, i.e., a gastropod or bivalve) in which asexual reproduction takes place and a vertebrate final host (e.g. fish, amphibians, birds, or mammals), where sexual reproduction and egg production occurs (Werding, 1969). Many

trematode taxa also require a second intermediate invertebrate or vertebrate host in which they form resilient and often encysted waiting stages, the metacercaria. Transmission between hosts occurs either actively, during a free-living larval stage where cercariae actively seek to enter their intermediate host, or passively, where encysted metacercaria await trophic transmission through consumption of the intermediate host by the final host (Combes et al., 1994; Lefebvre & Poulin, 2005; Marcogliese, 2004; Morley, 2012). Life cycle complexity, the number of intermediate hosts, and host specificity are species-dependent (Galaktionov & Bustnes, 1999; Puljas & Burazin, 2022; Werding, 1969). Environmental conditions can also determine which life cycle strategies are advantageous, as trematode species with no or only one free-living stage could have a higher chance of survival in harsher climates, because the direct impact of environmental stressors is reduced (Galaktionov & Bustnes, 1999; Galaktionov et al., 2015). This suggests a competitive advantage for species with shorter life cycles under certain conditions.

Because blue mussels are sessile and serve as first or second intermediate hosts for trematodes, they are a common model species to study parasite distribution and ecology along North-Atlantic coastlines (e.g. Brenner et al., 2014). For example, parasite prevalence and infection intensity can be used to estimate the possible effects trematodes can have on their host population and connected ecosystems (e.g. Bush et al., 1997; Marcogliese, 2004; Selbach et al., 2020). Other studies suggests that some trematodes, such as *Renicola parvicaudatus*, *Gymnophallus bursiculosa*, and *Himasthla* spp. can be expected to parasitize blue mussels in Arctic Norway (i.e. Galaktionov et al., 2015; Benito et al., 2022, 2023). However, little is known about the distribution, seasonal dynamics, host transmission, and specific behavior and development of these trematodes in the Arctic as most information derives from central European studies, and only a few recent studies have been conducted in the Norwegian Arctic (Benito et al., 2022, 2023; Galaktionov et al., 2015; Galaktionov & Bustnes, 1999).

Four key factors can be considered to determine and influence the temporal and spatial distribution of trematode communities and their interactions with ecosystems: abiotic and biotic factors, seasonality, and behavioral adaptations. Firstly, biotic interaction within their respective ecosystems can strongly impact trematode abundance. When assessing parasite abundance in blue mussels, it is crucial to consider interactions between parasites, intermediate hosts, final hosts, and their role within the food web. Bird abundance, for instance, greatly impacts parasite presence and abundance, as the distribution of trematodes often takes place via a mobile final host (e.g. Byers et al., 2008; Hilgerloh, 1997; Horn, 2017). These biotic factors

can also be affected and modulated by human influence. For instance, Galaktionov et al. (2015) found a threefold increase in several parasite species near fish farms compared to natural sites and linked their occurrence to increased numbers of their final hosts, seagulls. As anthropogenic influences, such as fisheries and aquaculture are continuously growing, human effects should be taken into consideration when investigating parasite communities in northern Norway (Espinasse et al., 2023).

Secondly, abiotic factors can affect trematode distribution, abundance, and heterogeneity (Bommarito et al., 2021). Especially the parasites' free-swimming stage are highly susceptible and vulnerable to environmental factors. Environmental stressors such as temperature, wave exposure, salinity, pH, and light dictate cercariae survival directly, and certain trematode species are better adapted to harsher conditions by reducing the time exposed to these stressors (Combes, 1994; Marcogliese & Cone, 1997; Nikolaev et al., 2017). Additionally, environmental stressors not only impact the parasites directly but can affect the different host species, and thus also indirectly determine trematode distribution, infection intensity, and prevalence (Cornelius, et al., 2023). As abiotic factors can vary greatly in the diverse habitats of northern Norwegian coastal ecosystems, differences between locations should be monitored at a small scale when investigating parasite communities.

Thirdly, seasonal variation impacts trematode communities, as seasonality strongly drives abiotic and biotic factors, especially in extreme environments (Studer & Poulin, 2012, Svärth, 1999). Temperature changes accompanying seasonality might influence parasite and host behavior and the Arctic climate reaches extremes in terms of duration and absolute low temperatures. Thieltges & Rick (2006) found differences in encystment and emergence of parasite transmission stages based on temperature and seasonality. In the Arctic, however, diverging results, with lower temperatures preferred for cercariae emergence than in central European habitats have been observed, even for closely related species (see Galaktionov et al., 2015). Monitoring changes in trematode communities and abundance throughout the seasons could give a better indication of seasonal dynamics. Additionally, exceptionally short vegetation periods and harsh winters could favor certain life history strategies unique to this environment (Bush et al., 1997; Walsh, 2008).

Lastly, behavioral adaptations to the biotic, abiotic, and seasonal factors could be reflected in transmission strategies that maximize infection success in the parasites' target host. For example, Fingerut et al. (2003) observed patterns of dispersal in *Himasthla* sp. along an

intertidal gradient or microhabitat to bottom layers, guided through geo- and phototaxis. *Renicola* sp., on the contrary, emerges to the water surface, allowing for wider dispersal after emergence from their first intermediate host (Galaktionov et al., 2015; Thieltges & Reise, 2007; Prinz et al., 2011; Nikolaev, 2017). This behavior indicates a preference for a position within the intertidal zone in trematodes and might additionally be advantageous depending on the trematodes' preferred final host (Krapivin et al., 2018). As cercariae only have a limited time window to find a suitable host to complete their transmission, this behavior must increase trematode fitness and it can be assumed that patterns of distribution should be observable along the intertidal gradient (Combes et al., 1994; Krapivin et al., 2018; Nikolaev et al., 2017). For example, a greater abundance of *Gymnophallus* spp. was found in subtidal areas while *R. roscovita* was found predominantly in the intertidal zone, reflecting the parasite's final hosts, diving ducks and gulls, respectively (Krapivin et al., 2018). These findings indicate clear patterns of species distributions, possibly due to behavioral adaptations. Accumulation at certain positions within the intertidal zone could give information about the final host choice of trematodes and document behavioral patterns of trematode communities in Arctic Norway (Combes, 1994).

While trematode abundance in *Mytilus* spp. is well documented and studied in lower latitudes (e.g. Lauckner, 1983), little information is available from northern ecosystems (e.g. Benito et al., 2023; Galaktionov et al., 2015; Galaktionov & Bustnes, 1999). In addition, many studies have either investigated larger latitudinal spans (e.g. Benito et al., 2022) or looked exclusively at small-scale intertidal differences (e.g. Nikolaev et al., 2017). At the same time, clustering around human-made structures has been observed (Galaktionov & Bustnes, 1999). However, the extent to which spatial divergence of different levels plays a role in trematode community composition has not yet been fully explored. Abundance, community composition, and seasonal variation need further exploration in Arctic ecosystems at a closer spatial scale.

In this thesis, I will describe the trematode community in blue mussels *Mytilus* spp. in rocky intertidal systems in Arctic Norway. As elaborated above, there is still great uncertainty around trematode and host distribution, community structure, life cycles, and the determining biotic and abiotic factors in high-latitude regions. My thesis will therefore focus on describing present trematode communities, using infection intensity and prevalence in Arctic blue mussels at different temporal and spatial scales (Bush et al., 1997). I will do so by taking four key factors influencing trematode communities into account: (i) anthropogenic influences on trematode

communities within blue mussels by comparing populations under low and high human influence; (ii) abiotic influence by testing for differences between wave-exposed and wave-sheltered microhabitats; (iii) trematode distribution along the intertidal gradient; and (iv) seasonal effects on Arctic trematode communities. The following hypotheses will be tested:

(H1) Anthropogenic influence increases trematode infection rates in Arctic blue mussels.

(H2) Reduced wave exposure will increase the infection rates of trematodes in Arctic blue mussels.

(H3) Trematode communities in Arctic blue mussels display differences along the intertidal gradient.

(H4) Seasonality affects patterns of Arctic trematode communities in blue mussels, with increases in infection rates after infection taking place throughout the vegetative period.

By incorporating this multi-dimensional approach in host sampling, I intend to provide a holistic overview of trematode communities in Arctic blue mussels across seasons and various spatial scales.

2. Material and Methods

2.1 Site Description

Sommarøy area is situated off the southwest coast of the Island of Kvaløya in Troms County in northern Norway (Figure 1). It is located approximately 60 km southwest of the city of Tromsø. The climate in the area is subarctic, with average temperatures for the region of 2.92 degrees Celsius (°C) and precipitation at 1018 millimeters (mm) (Thornsnæs et al., 2023). The highest and lowest temperatures recorded were 30.4°C and -22°C in 2014 and 1910, respectively. Salinity is measured between 26 and 37 Practical Salinity Units (PSU) (Appendix 1).

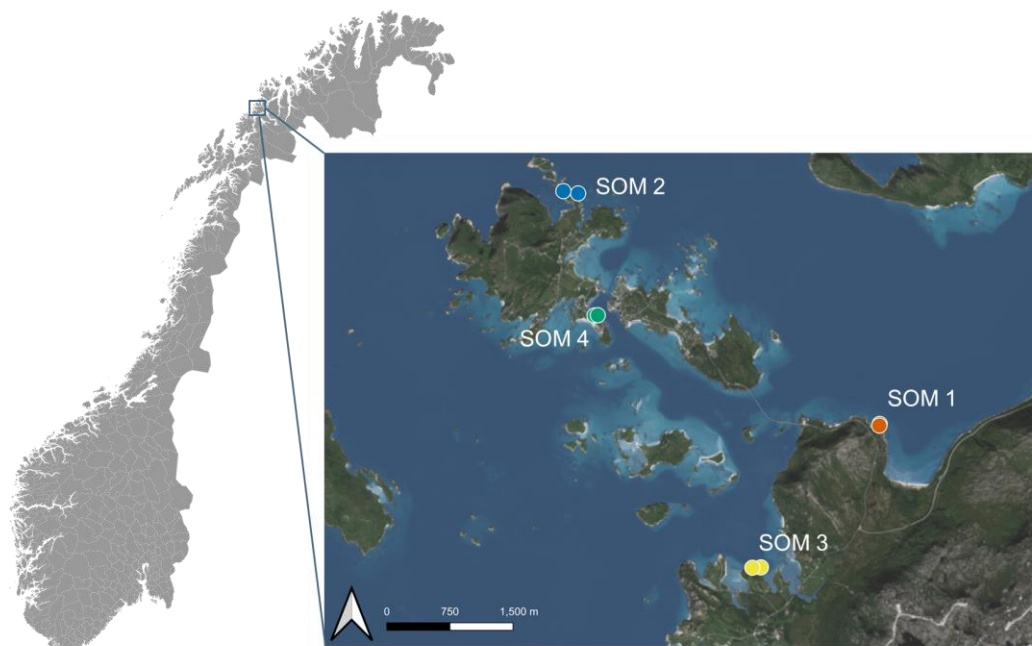


Figure 1 - Overview of sampling locations SOM1 (orange), SOM2 (blue), SOM3 (yellow), and SOM4 (green) in the Sommarøy area close to Tromsø, using NorgeiBilder as a Background map.

Two natural sampling locations were selected at the northern waterfront of the area, based on their remoteness from human disturbance. SOM1, near Sandvikssletta Beach (69° 62'N, 18°08'E) and SOM2, on Hillesøya (69°65'N, 17°99'E). Human-influenced locations were situated on at the fish-processing plant *Ivan Lorentzen Fiskeforretning AS* located on the east coast of Kvaløya, SOM3 (69°61'N, 18°04'E) and the south-facing side, in the harbor area, SOM4 (69°63'N, 17°99'E). At each location, a wave-exposed site and a wave-sheltered site were selected (< 200 m apart), making up a total of eight sites (Figure 2). Wave-sheltered sites were chosen based on visual differences in water movement and a great abundance of *Ascophyllum nodosum* was used as an indicator for reduced wave exposure.

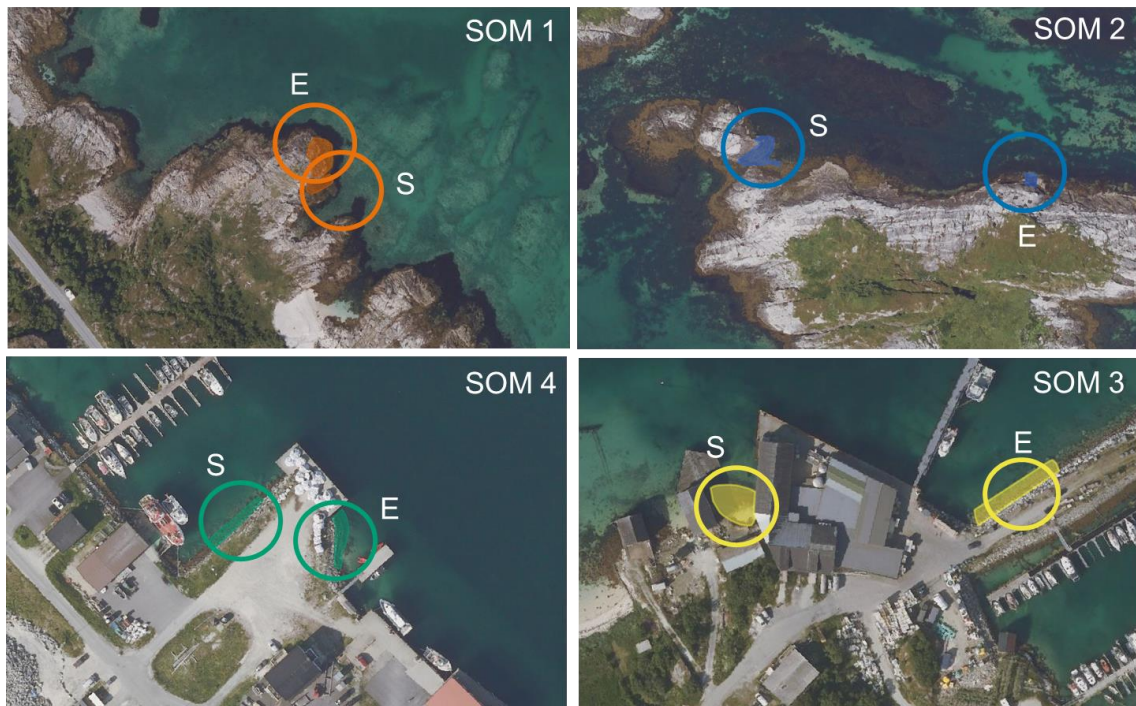


Figure 2 – Close-up overview of the sample locations. At all four locations (natural SOM1 (orange) & SOM2 (blue); human-influenced SOM3 (yellow) & SOM4 (green)), a wave-sheltered (S) and a wave-exposed (E) site was selected.

To test for the distribution of trematode infections along an intertidal gradient, four levels were selected at the wave-exposed sites SOM1E and SOM2E. The area between the lowest low tide and the highest border of the intertidal zone (barnacle growth) was divided into four segments, ‘top’, ‘high’, ‘mid’, and ‘low’.

Detailed site descriptions took place throughout the sampling process which assessed species presence, wave exposure, substrate, and human influence (Table 1). The distance to the closest human construction was measured using QGIS Firenze 2.8.

Table 1 - Detailed site description including human influence, wave exposure (Wave-exposed E, Wave-sheltered S), substrate, and coordinates for all sampling sites.

| Location | Site | Human influence | | Substrate | | Coordinates | |
|----------|--------|-----------------|---------------------------------|------------------|------------------|-------------|----------|
| | | Human influence | Distance to human structure (m) | Substrate source | Type | Lat (°N). | Long(°E) |
| SOM1 | SOM1E* | low | 136 | natural | rocky intertidal | 69.621 | 18.082 |
| SOM1 | SOM1S | low | 152 | natural | rocky intertidal | 69.621 | 18.082 |
| SOM2 | SOM2E* | low | 490 | natural | rocky intertidal | 69.647 | 17.989 |
| SOM2 | SOM2S | low | 393 | natural | rocky intertidal | 69.647 | 17.989 |
| SOM3 | SOM3E | high | 0 | artificial | rocky breakwater | 69.606 | 18.043 |
| SOM3 | SOM3S | high | 0 | natural | rocky intertidal | 69.606 | 18.040 |
| SOM4 | SOM4E | high | 0 | artificial | rocky breakwater | 69.634 | 17.996 |
| SOM4 | SOM4S | high | 0 | artificial | rocky breakwater | 69.634 | 17.996 |

*Sites were divided into top, high, mid, and low for analysis along the intertidal gradient

2.2 Sampling

2.2.1 Mussel Sampling

To compare the infection intensity and the infection prevalence between seasons, sampling took place from February 2023 until October 2023, once every season, i.e. in February (winter), May (spring), August (summer), and October (fall). During each sampling, mytilids with an approximate length between 1.5 and 4 centimeters (cm) were randomly selected and placed in labeled plastic bags. Samples were then stored at -18°C until further analysis.

Twenty *Mytilus* sp. were sampled at each site during winter. After observing a high variability in prevalence and infection intensity among the mussels sampled in winter, the sample size was increased to 40 individuals per site for spring, summer, and fall samplings. For analysis along the intertidal gradient, 20 mussels were sampled per intertidal level in winter and 40 mussels during fall for each intertidal level at SOM1E and SOM2E.

Because the locations SOM3 and SOM4 did not display differences in wave exposure to the same degree as the natural locations SOM1 and SOM2, the human-influenced locations were excluded from further analysis of wave exposure.

2.2.2 Additional Biodiversity Assessments

In addition to mussel sampling, biotic factors potentially influencing trematode abundance were assessed. Snail density was assessed inside a 50*50 cm frame, randomly placed at two areas within each site during each sampling (winter, spring, summer, and fall). All snails were removed from the 50*50 cm area, photographed on a tray, and then released back at the site. Images were then examined to count the snails and identify the species. Algae and lichens at the sites were identified during mussel sampling and visually identified to species level.

2.3 Mussel Dissection and Parasite Identification

Mussels were taken out of the freezer and thawed for a minimum of 45 minutes before dissection. Closed mussels were measured from the umbo along the anterior-posterior axis in length by using a digital caliper with a precision of 0.01 cm (Cocraft, Sweden) and stored in labeled plastic bags until further analysis. Valves were opened by cutting through the abductor muscle using a scalpel and scraping out the soft parts of the mussel. Mussel flesh was then squeezed between two plexiglass plates.

Each mussel was screened for trematodes using a Leica M125 C Stereomicroscope (Leica Microsystems, Germany), and the number of trematodes as well as the tissue of occurrence (foot, mantle, gills, intestine, or other) was recorded. Parasites were morphologically identified based on keys and descriptions (Galaktionov et al., 2023; Cremonte, 2015, Benito, 2022)

The presence of other organisms and particles, such as pearls, plastic particles, copepods, pearls, or nematodes was documented. Larger pearls, hindering the squeezing process, were removed, and the number of pearls was noted down.

2.4 Statistical Analysis of Trematode Data

Statistical testing was performed using R Statistical Software (v 4.3.1; R Core Team 2021). Results were deemed significant with a threshold of $\alpha < 0.05$ for both infection intensity and prevalence. The data was visualized using the ‘ggplot2’ package (Wickham, 2016).

Data were divided into appropriate data frames for each hypothesis as described below. Each hypothesis was tested using appropriate models for both infection intensity and prevalence (Table 2). The same predictor variables were used for both models and trematode species (see below) and comparisons between predictor variables were achieved using the *relevel()*-function. Mussel length (mm) was included as a covariable variable in all models to account for possible variation due to mussel size.

Statistical analysis can be reproduced using https://github.com/FDR1204/Master_FDR_UiT.

2.4.1 Infection Intensity

To analyze the infection intensity of *Renicola* sp. and *Gymnophallus* sp. in blue mussels, a zero-truncated negative binomial generalized linear model was used (package ‘VGAM’, Yee, 2024). Count data of each trematode species from infected mussels only were used for testing infection intensity. The negative binomial distribution (family = posnegbinomial) with a ‘log’ link was selected to account for overdispersion and the exclusion of zeros. To validate underlying model assumptions, residuals were assessed using the *plot()*-function.

For testing the effects of location (Hypothesis 1) and season (Hypothesis 4), the data included all locations and all seasons (number of mussels infected with *Renicola* sp. = 1251; number of mussels infected with *Gymnophallus* sp. = 786). For wave exposure (Hypothesis 2), the data included only samples from locations SOM1 and SOM2 (number of mussels infected with *Renicola* sp. = 932; number of mussels infected with *Gymnophallus* sp. = 519). When assessing

differences along the intertidal zone (Hypothesis 3), the data included only winter and fall samples from SOM1E and SOM2E (number of mussels infected with *Renicola* sp. = 482; number of mussels infected with *Gymnophallus* sp. = 287).

For hypotheses one and four, testing for the effects of location and seasonality respectively, the predictor variables were ‘season’, ‘location’, and ‘length’, and when the analysis included interactive effects, the interaction between ‘season’ and ‘location’ was included (Table 2). For hypothesis two, testing differences between wave-exposed and wave-sheltered sites, the predictor variables used were ‘wave-exposure’ and mussel ‘length’ (Table 2). When interactive effects were added to the model, the interaction between ‘wave-exposure’ and ‘location’, and the interaction between ‘wave-exposure’ and ‘season’ were analyzed in addition (Table 2). Lastly, when testing hypothesis three, differences between intertidal levels, the predictor variables used were ‘intertidal level’, and ‘length’, and when including interactive effects, the interaction between ‘intertidal level’ and ‘location’, and the interaction between ‘intertidal level’ and ‘season’ were added (Table 2).

Table 2 - Overview of models used for statistical analyses. Analysis was conducted on both, *Renicola* sp. and *Gymnophallus* sp., which were treated as a response variable. Predictor variables were chosen model-specific. For infection intensity, the number of trematodes within infected blue mussels was used. For infection prevalence, infected (1) -uninfected (0) data of sampled blue mussels were used.

| Predictor variables | Family function | Link function | Appendix |
|--|-----------------|---------------|----------|
| Infection intensity (vglm) | | | |
| Hypothesis 1 & Hypothesis 4 | | | |
| * Season+Location+Length | Posnegbinomial | ‘log’ | 4; 11 |
| ** Season+Location+Length+Season*Location | Posnegbinomial | ‘log’ | 5; 12 |
| Hypothesis 2 | | | |
| * Wave_exposure+Length | Posnegbinomial | ‘log’ | 7; 14 |
| ** Season+Location+Length+Season*Wave_exp.+Location*Wave_exp. | Posnegbinomial | ‘log’ | 8; 15 |
| Hypothesis 3 | | | |
| * Intertidal_level+Length | Posnegbinomial | ‘log’ | 9; 16 |
| ** Intertidal_level+Length+Season*Int_level+Location*Int_level | Posnegbinomial | ‘log’ | 10; 17 |
| Infection prevalence (glm) | | | |
| Hypothesis 1 & Hypothesis 4 | | | |
| * Season+Location+Length | binomial | ‘logit’ | 19; 25 |
| ** Season+Location+Length+Season*Location | binomial | ‘logit’ | 20; 26 |
| Hypothesis 2 | | | |
| * Wave_exposure+Length | binomial | ‘logit’ | 21; 27 |
| 21** Season+Location+Length+Season *Wave_exp.+Location*Wave_exp. | binomial | ‘logit’ | 22; 28 |
| Hypothesis 3 | | | |
| * Intertidal_level+Length, | binomial | ‘logit’ | 21; 29 |
| ** Intertidal_level+Length+Season*Int_level+Location*Int_level | binomial | ‘logit’ | 24; 30 |

* = base model

** = model including interactive effects

2.4.2 Prevalence

For prevalence, count data of infecting trematodes within each sampled mussel were converted to binary data (1 = infected; 0 = uninfected). The prevalence of infections with *Renicola* sp. and *Gymnophallus* sp. was analyzed as infection likelihood using a logistic regression model. The analysis employed the binomial family function and the ‘logit’ link function within a generalized linear model (GLM) framework. The package DHARMA was used to analyze the residuals to ensure a good model fit (Hartig, 2022).

For seasonality and location, the entire dataset was used for both species tested (number of mussels for both trematodes = 1557). When testing for differences in wave exposure, only data from locations SOM1 and SOM2 were used for both trematodes (number of mussels for both trematodes = 996). The same predictor variables for all three hypotheses were used as described for infection intensity (Table 2). The effect of position in the intertidal zone was tested using data from before and after the growing season (winter and fall) from natural exposed sites only. Infected-uninfected data for both trematodes were used (number of mussels for both trematodes = 521), and the same predictor variables were used as in the infection intensity analysis.

2.5 Additional Biodiversity Data Processing

To assess the effects of biotic factors on trematode communities, data on the first and final hosts of the trematodes (snails and birds respectively) and algae and lichen communities in the area were assessed. Photographed snails were counted and identified to species level to calculate the density of each species for each site. Four snail species were identified: *Nucella lapillus* (Linnaeus, 1758), *Littorina obtusata* (Linnaeus, 1758), *Littorina saxatilis* (Olivi, 1792), and *Littorina littorea* (Linnaeus, 1758). Due to morphological similarities, *L. saxatilis* and *L. littorea* were grouped.

Bird data was accessed through Artskart, the Norwegian Species Database (accessed 13.04.2024). Data from the taxon ‘Fugler’ (Norwegian: Birds) was selected from the Sommarøy area and analyzed in QGIS Firenze 2.8 software (QGIS Development Team, 2015). Sighting describes one or more individuals of a bird species, including the coordinates of the sighting. At each site, recorded sightings were selected in a radius of 1000 m using the ‘buffer’ function. Data from both sites at each location were then combined to retrieve bird sightings in a 1000 m radius of each location. The ‘clip’ function was used to select the data points. Selected

data points were then exported and further analyzed in R Statistical Software (v 4.3.1; R Core Team 2021). Species recorded during each sighting were assigned to their functional group, of either 'Ducks', 'Gulls', 'Waders', or 'Others' manually to gain an overview of the bird functional groups at each location. Differences in bird composition were based on these groups and visually analyzed. All figures were created using 'ggplot2' in R (Wickham, 2009).

Algae and lichen species richness at each site was assessed. Present species at each location were compared as a biodiversity measure for each subgroup (brown algae, green algae, red algae, and lichens) as well as overall species richness.

3. Results

3.1. Trematode Infections

A total of 1557 *Mytilus* sp. were screened for trematode infections. Metacercariae of three trematode species *Gymnophallus* sp., *Himasthla* sp., and *Renicola* sp. were found (Figure 3). The overall prevalence and mean infection intensity were 76.04% and 16.40 for *Renicola* sp. and 49.36% and 2.94 for *Gymnophallus* sp. respectively. *Himasthla* sp. was only found in two blue mussels and is therefore excluded from further analysis. Table 3 provides an overview of the prevalence and infection intensities at the different locations and sites.

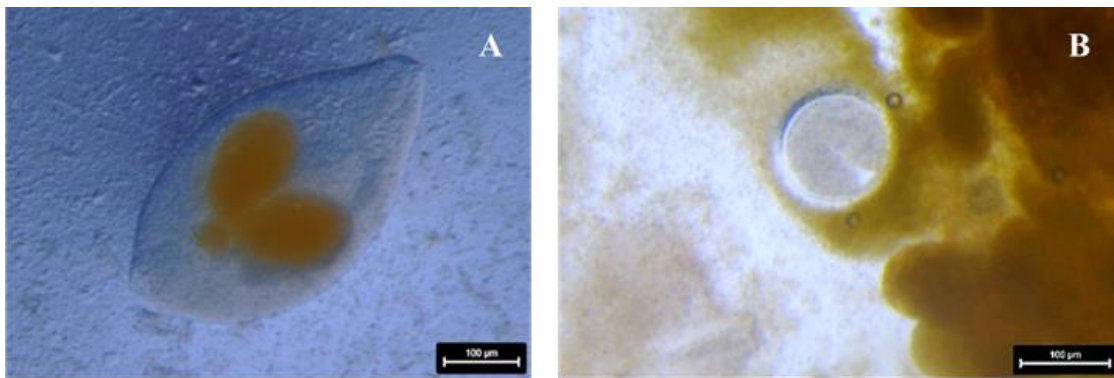


Figure 3 – A) Metacercaria of *Gymnophallus* sp., ventral view. **B)** Metacercaria of *Renicola* sp.

Based on previous studies in this area, it can be assumed that the species found in this study are *Renicola parvicaudatus* (Stunkard & Shawn, 1931), syn. *Renicola roscovitus* (Stunckard, 1932) (Galaktionov et al., 2015; Benito et al., 2018) possibly synonym *Cercaria parvicaudata* (Mehlis, 1831) (Appendix 2; Werding, 1969, WoRMS Editorial Board, 2024). However, for identification to the species level, further molecular analysis is necessary and the trematode will therefore be referred to as *Renicola* sp. (Figure 3A). In previous studies from Arctic regions, *Gymnophallus* sp. has been identified as *Gymnophallus bursiculosa* (Odhner, 1906) (Benito et al., 2023, Galaktionov, 2015), but will be referred to here as *Gymnophallus* sp. due to the lack of molecular confirmation of the samples in this study (Figure 3B, Appendix 3). The morphology of the trematode varied greatly in the samples of this study, possibly because of different developmental stages. Furthermore, gymnophalloids within brown mucus envelopes were observed, which are possibly mucoid envelopes surrounding the non-encysted cercariae, produced by the mussel as a defense mechanism (Cable, 1953; Lauckner, 1983). All differences described below were statistically significant according to the models described in Table 2 and releveling of factors took place to obtain pairwise comparisons between all predictor variables.

Table 3 - Prevalence and infection intensity for both, *Renicola* sp. and *Gymnophallus* sp. Results are displayed showing the number of mussels sampled, prevalence (%), mean infection intensity, including standard deviation (SD) and minimum-maximum values.

| Site | N | <i>Renicola</i> sp. | | | | <i>Gymnophallus</i> sp. | | | |
|-------|-----|---------------------|-----------|-------|------------|-------------------------|-----------|------|------------|
| | | Prevalence (%) | Intensity | | | Prevalence (%) | Intensity | | |
| | | | Mean | SD | Min.- Max. | | Mean | SD | Min.- Max. |
| SOM1E | 342 | 89.5 | 15.3 | 23.19 | 1-271 | 54.1 | 3.29 | 2.87 | 1-22 |
| SOM1S | 148 | 98.6 | 31.24 | 31.03 | 1-218 | 60.1 | 3.09 | 2.75 | 1-16 |
| SOM2E | 349 | 93.7 | 16.71 | 24.72 | 1-210 | 53.3 | 2.53 | 2.29 | 1-12 |
| SOM2S | 157 | 97.5 | 43 | 53.36 | 1-300 | 37.6 | 2.24 | 1.91 | 1-13 |
| SOM3E | 134 | 77.6 | 8.62 | 10.13 | 1 - 62 | 47.8 | 2.47 | 2.64 | 1-16 |
| SOM3S | 140 | 89.3 | 13.56 | 26.18 | 1-249 | 37.1 | 2.40 | 1.77 | 1-09 |
| SOM4E | 151 | 35.8 | 2.8 | 2.52 | 1-200 | 55.6 | 4.68 | 5.57 | 1-32 |
| SOM4S | 136 | 26.5 | 6.17 | 18.37 | 1-111 | 49.3 | 2.79 | 2.29 | 1-13 |

3.1.1 Infection Intensity

Renicola sp.

Effect of location and season - Infection intensity of *Renicola* sp. differed between all locations (Figure 4, Tabel 4i, Appendix 4). The smallest difference in infection intensity with *Renicola* sp. was between both natural locations, with SOM2 displaying only a slightly higher infection intensity than SOM1 (Tabel 4i, Appendix 4). Both natural locations displayed higher infection intensities compared to both human-influenced locations (Figure 4, Tabel 4i, Appendix 4).

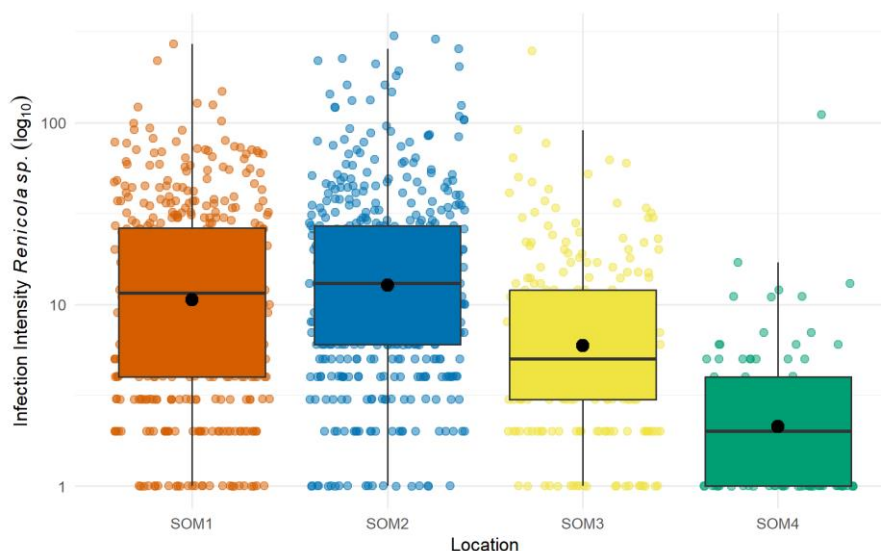


Figure 4 – Infection intensity of *Renicola* sp. for all seasons combined at different locations (SOM1 orange, SOM2 blue, SOM3 yellow, SOM4 green) displayed in boxplots on a log₁₀ scale. The vertical line within each boxplot represents the median at that location, and the dark point indicates the mean. Each point in the scatterplot represents the infection intensity for an individual sampled blue mussel.

Seasonality affected the infection intensity of *Renicola* sp. (Figure 5, Table 4ii, Appendix 4). The model identified the lowest infection intensity of *Renicola* sp. during winter, after taking the variation explained by mussel length into account (Table 4i, Appendix 4). Thereafter, an increase in infection intensity in fall took place (Table 4ii, Appendix 4). When analysis of infection intensity with *Renicola* sp. included the interaction effect of season and location, a general pattern of high infection intensity at natural locations and lowest infection intensity at SOM4 throughout all seasons, with an increase in infection intensity during fall could be observed (Appendix 5, 6).

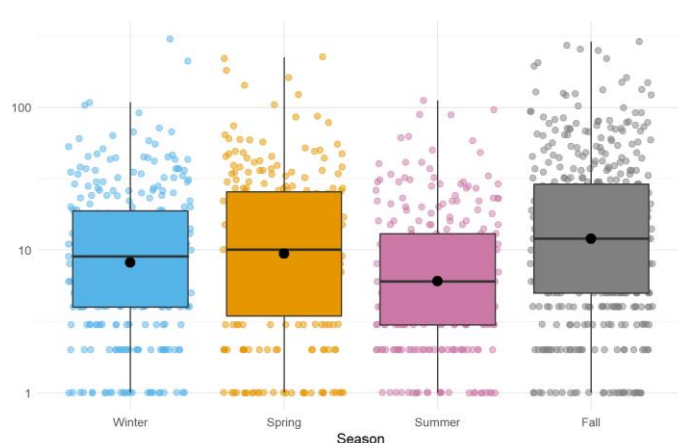


Figure 5 - Infection intensity of *Renicola* sp. for all locations combined at different seasons (Winter blue, Spring orange, Summer pink, Fall grey) displayed in boxplots on a log10 scale. The vertical line within each boxplot represents the median at that location, and the dark point indicates the mean. Each point in the scatterplot represents the infection intensity for an individual sampled blue mussel.

Table 4 – Pairwise comparisons of infection intensity of *Renicola* sp. based on a zero truncated negative binomial generalized linear model showing differences between sampling locations and among seasons. The table displays a combination of different outputs from the same model, obtained by releveling the factors. Values given are (from left to right): model estimate; standard error, z-value, and p-value. Statistically significant results where $p \geq 0.05$ are indicated in bold.

| vglm(Renicola_sp.~Location+Season+Length,family=posnegbinomial(),data) | | | | |
|--|--------------|-------------|---------------|------------------|
| i. Location - Location | Estimate | Std. Error | z value | Pr(> z) |
| SOM1 - SOM3 | -0.71 | 0.11 | -6.30 | <0.001 |
| SOM1 - SOM2 | 0.26 | 0.08 | 3.06 | 0.002 |
| SOM1 - SOM4 | -1.90 | 0.16 | -11.66 | <0.001 |
| SOM2 - SOM3 | -0.96 | 0.11 | -8.91 | <0.001 |
| SOM2 - SOM4 | -2.16 | 0.16 | -13.54 | <0.001 |
| SOM3 - SOM4 | -1.19 | 0.16 | -7.26 | <0.001 |
| ii. Season - Season | | | | |
| fall - spring | -0.20 | 0.10 | -1.92 | 0.054 |
| fall - summer | -0.21 | 0.12 | -1.79 | 0.074 |
| fall - winter | -0.45 | 0.10 | -4.56 | <0.001 |
| winter - summer | 0.24 | 0.12 | 2.04 | 0.042 |
| winter - spring | 0.25 | 0.11 | 2.25 | 0.024 |
| summer - spring | 0.01 | 0.12 | 0.09 | 0.925 |

Effect of wave exposure - The infection intensity of *Renicola* sp. was significantly higher at wave-sheltered sites compared to wave-exposed sites when combining both natural locations (Figure 6, Appendix 7). When including the interactive effects of location and wave exposure as well as season and wave exposure, individual differences in infection intensity with *Renicola* sp. were detected between locations and seasons, however, wave-sheltered sites almost always displayed a higher infection intensity than wave-exposed sites (Appendix 8, 9).

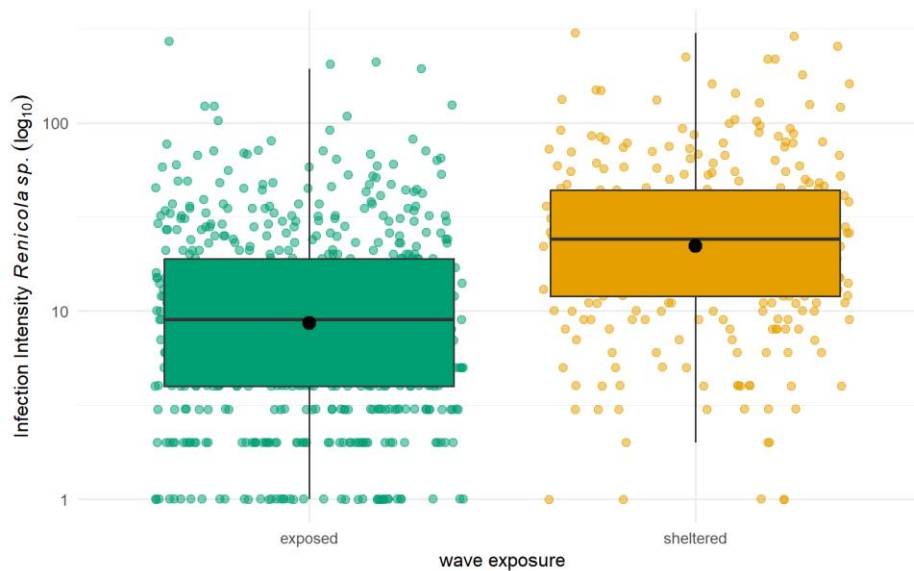


Figure 6 - Infection intensity of *Renicola* sp. at wave-exposed (green) and wave-sheltered (orange) sites (Locations SOM1 and SOM2 combined) displayed in boxplots on a \log_{10} scale. The vertical line within each boxplot represents the median, and the dark point indicates the mean. Each point in the scatterplot represents the infection intensity for an individual sampled blue mussel.

Effect of intertidal level - When analyzing differences in infection intensity of *Renicola* sp. between different levels along the intertidal zone at wave-exposed natural sites, a decrease in infection intensity with increasing intertidal level was found (Figure 7, Appendix 10). Specifically, both level 'top', and level 'high' demonstrated lower infection intensity compared to both the 'low' and 'mid' levels (Appendix 10). In addition, level 'mid' displayed lower infection intensity than level 'low' (Appendix 10). When analysis included the interactive effects of seasonality and intertidal level, as well as location and intertidal level on the infection intensity of *Renicola* sp., a general trend of decreasing infection intensity with increasing intertidal level, with some specific deviations based on location, intertidal level, and season was found (Figure 8, Appendix 11).

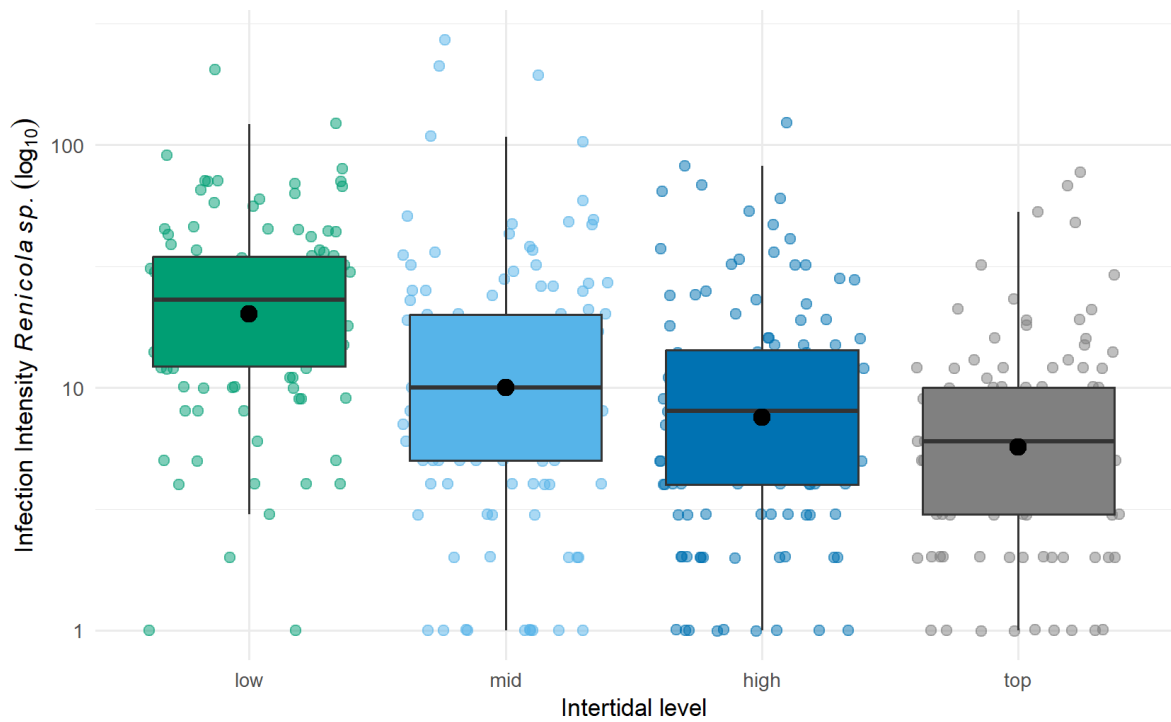


Figure 7 - Infection Intensity of *Renicola* sp. distributed along the intertidal gradient at natural, wave-exposed site combined, ascending from levels 'low' to 'top' on a \log_{10} scale ('low' green, 'mid' light blue, 'high' dark blue, 'top' grey). Displayed in a histogram with individual samples plotted with colored dots. The black line represents the median while the black dots represent the mean infection intensity at each intertidal level.

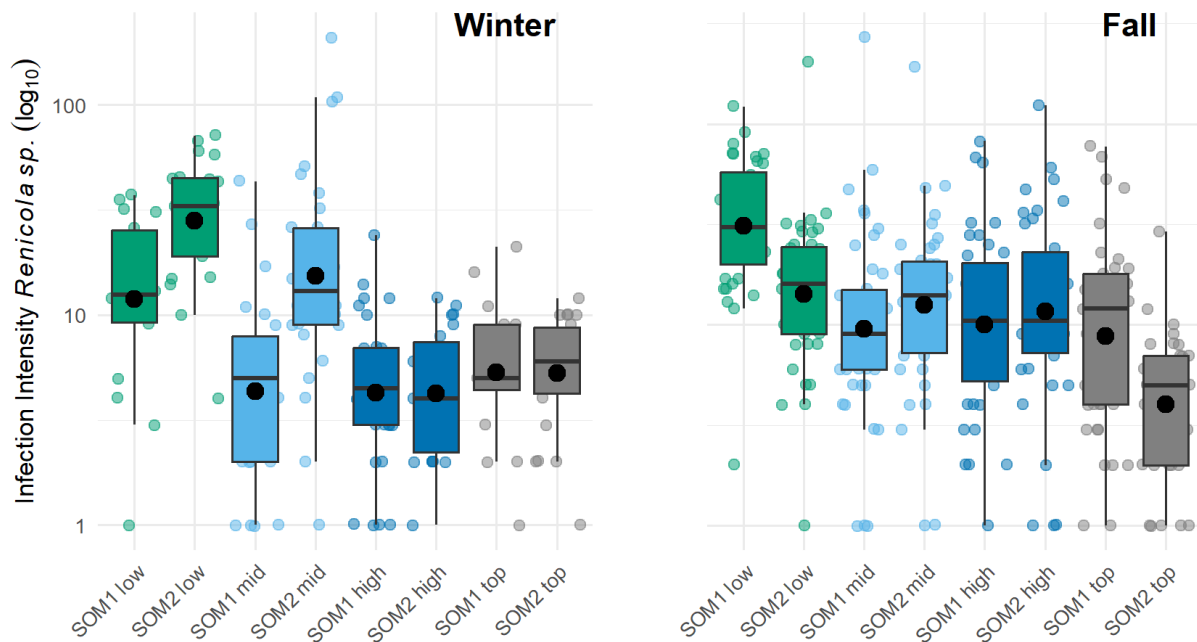


Figure 8 - Infection intensity of *Renicola* sp. distributed along the intertidal gradient at natural locations at exposed sites, showing sites and season, ascending from levels 'low' to 'top' on a \log_{10} scale ('low' green, 'mid' light blue, 'high' dark blue, 'top' grey). Displayed in a histogram with singular samples plotted with a colored dot. The black line represents the median while the black dots represent the mean infection intensity.

Gymnophallus sp.

Effect of location and season - *Gymnophallus* sp. showed some differences in infection intensity between locations (Figure 9, Tabel 5i, Appendix 12). SOM1 and SOM4 had a higher infection intensity than SOM2 and SOM3 (Figure 9, Table 5i, Appendix 12).

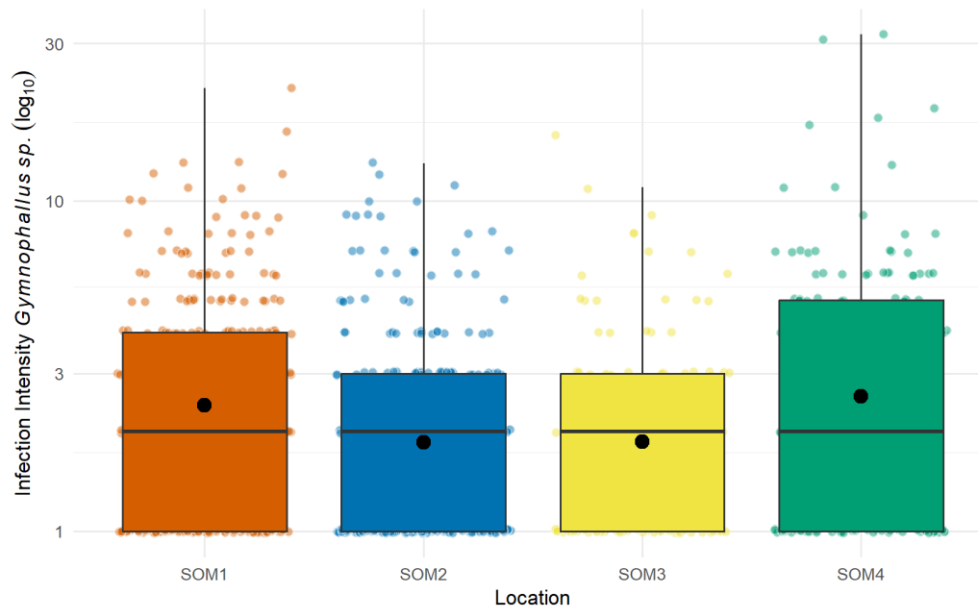


Figure 9 – Infection intensity of *Gymnophallus* sp. for all seasons combined at different locations (SOM1 orange, SOM2 blue, SOM3 yellow, SOM4, green) displayed in boxplots on a \log_{10} scale. The horizontal line within each boxplot represents the median infection intensity at that location, and the dark point indicates the mean infection intensity. Each point in the scatterplot represents the infection intensity for an individual sampled blue mussel.

Table 5 – Pairwise comparisons of infection intensity of *Gymnophallus* sp. based on a zero truncated negative binomial generalized linear model showing differences between sampling locations and among seasons. The table displays a combination of different outputs from the same model, obtained by releveling the factors. Values given are (from left to right): model estimate; standard error, z-value, and p-value. Statistically significant results where $p \geq 0.05$ are indicated in bold

| vglm(Gymnophallus_spp.~ Location+Season+Length,family = posnegbinomial(),data) | | | | |
|---|--------------|-------------|--------------|------------------|
| i. Location - Location | Estimate | Std. Error | z value | Pr(> z) |
| SOM1 - SOM2 | -0.47 | 0.13 | -3.54 | <0.001 |
| SOM1 - SOM3 | -0.49 | 0.18 | -2.80 | 0.005 |
| SOM1 - SOM4 | 0.22 | 0.16 | 1.34 | 0.181 |
| SOM2 - SOM3 | -0.02 | 0.18 | -0.13 | 0.893 |
| SOM2 - SOM4 | 0.69 | 0.16 | 4.21 | <0.001 |
| SOM3 - SOM4 | 0.71 | 0.19 | 3.83 | <0.001 |
| ii. Season - Season | | | | |
| fall - spring | 0.18 | 0.15 | 1.18 | 0.238 |
| fall - summer | -0.21 | 0.18 | -1.20 | 0.230 |
| fall - winter | 0.29 | 0.14 | 2.04 | 0.041 |
| winter - spring | -0.11 | 0.16 | -0.69 | 0.489 |
| winter - summer | -0.50 | 0.18 | -2.83 | 0.005 |
| spring - summer | -0.39 | 0.18 | -2.20 | 0.028 |

Infection intensity of *Gymnophallus* sp. differed between seasons (Figure 10, Tabel 5ii, Appendix 12). During winter, a higher infection intensity was observed compared to fall, and infection intensity during summer was lower compared to winter and spring (Table 5ii, Appendix 12). After including the interactive effect of seasonality and location the highest infection intensity with *Gymnophallus* sp. was generally found at SOM1 and SOM4, with some season and location-specific deviations from that trend (Appendix 13, 14).

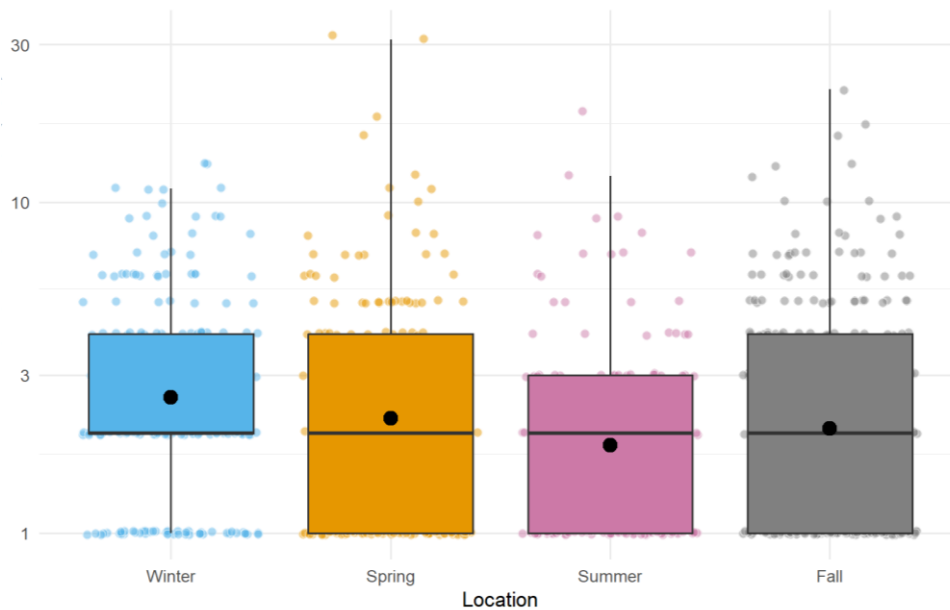


Figure 10 - Infection intensity of *Gymnophallus* sp. for all locations combined at different seasons (Winter blue; Spring orange; Summer pink; Fall grey) displayed in boxplots on a log₁₀ scale. The vertical line within each boxplot represents the median at that location, and the dark point indicates the mean. Each point in the scatterplot represents the infection intensity for an individual sampled blue mussel.

Effect of wave exposure - Infection intensity with *Gymnophallus* sp. did not differ between wave-exposed and wave-sheltered sites at natural locations (Appendix 15) When including the interactive effects of location and wave exposure as well as season and wave exposure on infection intensity with *Gymnophallus* sp., some differences were found (Appendix 16, 17).

Effect of intertidal level - Infection intensity of *Gymnophallus* sp. did not differ along the intertidal gradient (Appendix 18). Additionally, when looking at the interaction effects of location and wave exposure as well as seasonality and wave exposure, no differences in infection intensity were found for *Gymnophallus* sp. (Appendix 19).

3.1.2 Prevalence Analyzed as Infection Likelihood

Renicola sp.

Effect of location and season - The four locations display a similar pattern in the likelihood of infection of *Renicola* sp. as found for infection intensity (Figure 11, Table 6i, Appendix 20). No difference between locations SOM1 and SOM2 but differences among all other locations were identified (Table 6i, Appendix 20). A lower likelihood of infection at SOM3 and SOM4 was found compared the SOM1 and SOM2 (Figure 11, Table 6i, Appendix 20). SOM 4 displayed the lowest likelihood of infection (Figure 11, Table 6i, Appendix 20).

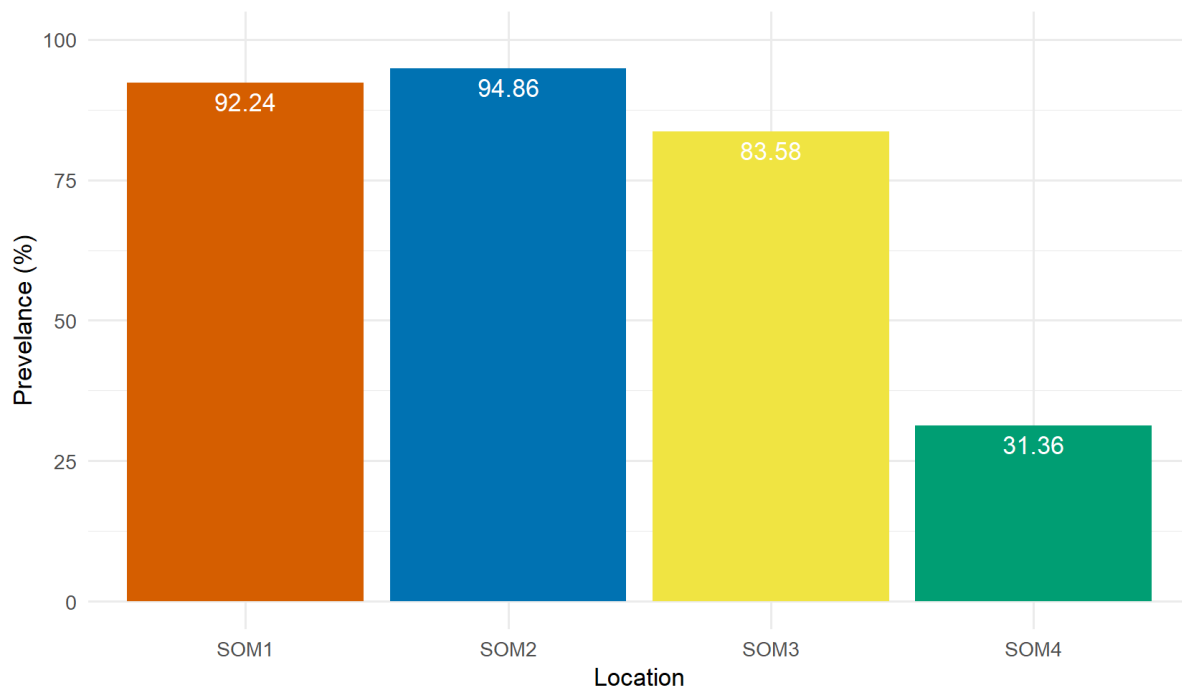


Figure 11 - Prevalence of *Renicola* sp. at each location (SOM1 orange, SOM2 blue, SOM3 yellow, SOM4 green) in percentages (%), averaged over seasons. Data are displayed in a bar chart with prevalence in percentages indicated in white.

Infection likelihood of *Renicola* sp. displayed differences in infection likelihood between seasons (Figure 12, Table 6ii, Appendix 20). Summer had a higher infection likelihood compared to all other seasons when including mussel length in the analysis (Table 6ii, Appendix 20). When including the interactive effect of location and season in the analysis of infection likelihood for *Renicola* sp., SOM1, and SOM2 generally displayed the highest while SOM4 had the lowest infection likelihood, although some individual differences between locations at different seasons were found (Appendix 21, 22).

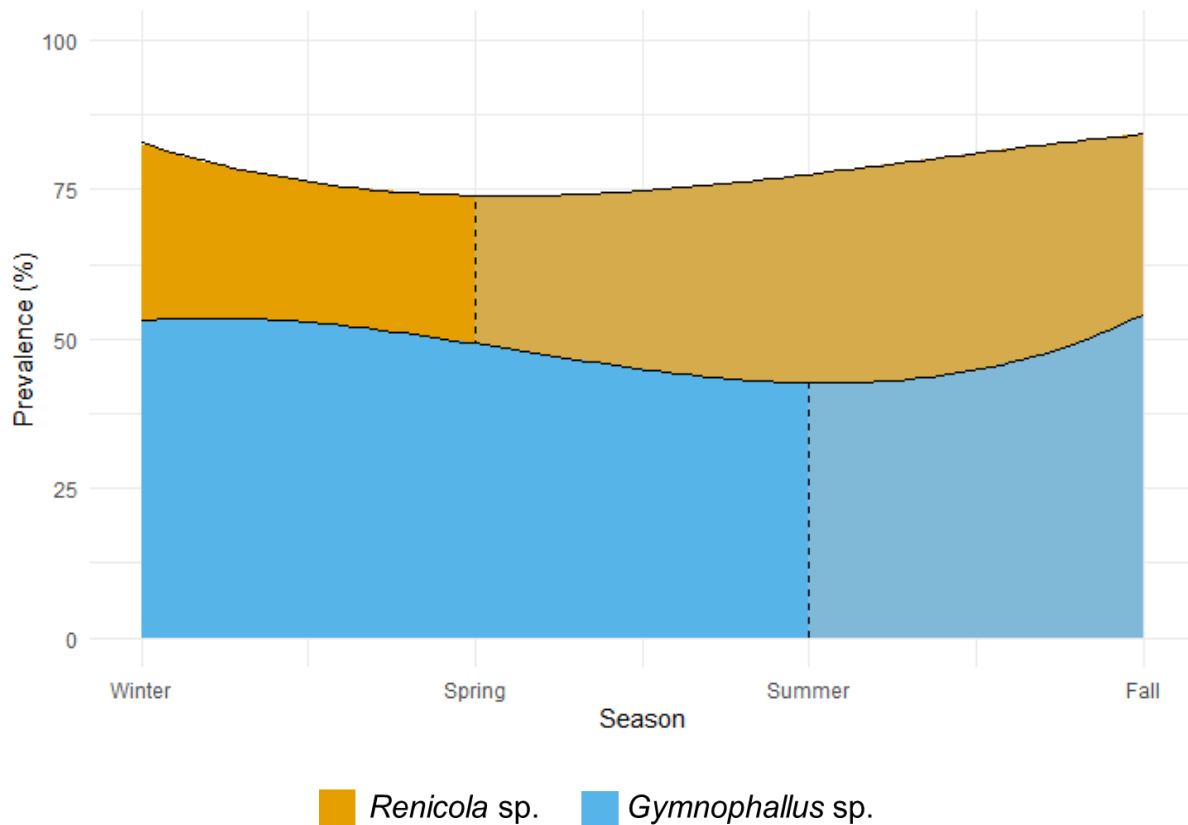


Figure 12 - Prevalence of infected mussels with *Renicola* sp. (orange) and *Gymnophallus* sp. (blue) throughout all seasons for all locations combined. Dotted lines and grey areas indicate an increase in prevalence after spring and summer for *Renicola* sp. and *Gymnophallus* sp. respectively, when visualizing the raw data.

Table 6 - Comparisons based on a generalized linear model showing differences in infection likelihood of *Gymnophallus* sp. between sampling locations and seasons. The table displays a combination of different outputs from the same model, obtained by releveling the factors. Values given are (from left to right): model estimate; standard error, z-value, and p-value. Statistically significant results where $p \geq 0.05$ are indicated in bold.

| glm(Renicola_sp._Bin ~ Location+Season+Length+Location*Season, family = binomial (link = "logit") ,data) | | | | |
|---|--------------|-------------|---------------|------------------|
| i. Location - Location | Estimate | Std. Error | z value | Pr(> z) |
| SOM1 - SOM3 | -1.20 | 0.26 | -4.69 | <0.001 |
| SOM1 - SOM2 | 0.32 | 0.27 | 1.19 | 0.233 |
| SOM1 - SOM4 | -3.78 | 0.26 | -14.74 | <0.001 |
| SOM2 - SOM3 | -1.52 | 0.27 | -5.61 | <0.001 |
| SOM2 - SOM4 | -4.10 | 0.26 | -15.50 | <0.001 |
| SOM3 - SOM4 | -2.59 | 0.22 | -11.90 | |
| ii. Season - Season | | | | |
| fall - spring | 0.03 | 0.24 | 0.12 | 0.902 |
| fall - summer | 0.65 | 0.26 | 2.50 | 0.013 |
| fall - winter | 0.07 | 0.24 | 0.28 | 0.779 |
| winter - summer | 0.58 | 0.25 | 2.29 | 0.022 |
| winter - spring | -0.04 | 0.24 | -0.15 | 0.878 |
| spring - summer | 0.62 | 0.24 | 2.59 | 0.009 |

Effect of wave exposure - The infection likelihood of blue mussels with *Renicola* sp. was higher at wave-sheltered sites compared to wave-exposed sites (Figure 13, Appendix 23). While

interactive effects between season and wave exposure as well as location and wave exposure showed higher infection likelihood at wave-sheltered sites, these effects were non-significant with one exception (Appendix 24, 25).

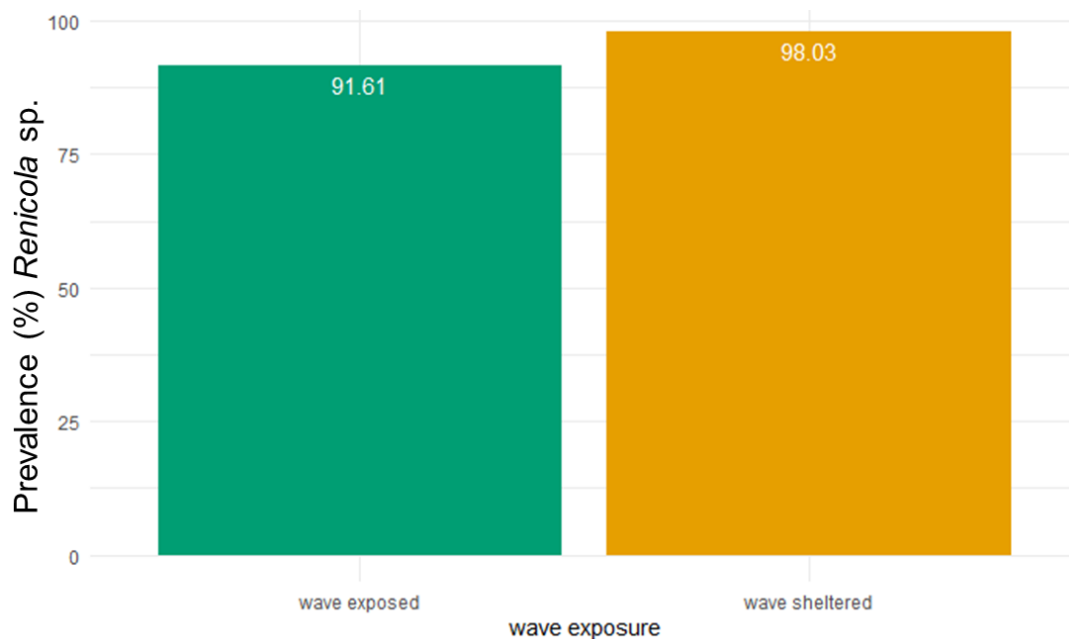


Figure 13 – Prevalence in percentage (%) of infected mussels *Renicola* sp. at wave-exposed (green) and wave-sheltered (orange) sites for both natural locations combined. Data are displayed in a bar chart with prevalence in percentages indicated in white.

Effect of intertidal level - Differences in the infection likelihood with *Renicola* sp. were found (Figure 13, Appendix 26). Level ‘mid’ had a higher infection likelihood than level ‘top’, after the model corrected infection prevalence for mussel size (Appendix 26). The interactions between season and intertidal level as well as location and intertidal level showed some individual differences between levels at different locations during winter and fall. However, generally, an increase with decreasing intertidal levels occurred (Appendix 27, 28).

***Gymnophallus* sp.**

Effects of location and season – Infection likelihood with *Gymnophallus* sp. differed between locations (Figure 14, Tabel 6i, Appendix 29). The infection likelihood was higher at SOM1 compared to SOM2 and SOM3 (Tabel 7i, Appendix 29). In addition, SOM4 displayed a higher infection likelihood than SOM3 (Tabel 7i, Appendix 29). When looking at the effect of season on infection likelihood with *Gymnophallus* sp., it was lower during summer than during fall and winter (Tabel 7ii, Appendix 29). When including the interactive effects of location and season, in the analysis of infection likelihood with *Gymnophallus* sp., some season-specific differences were found at the different locations (Appendix 30, 31)

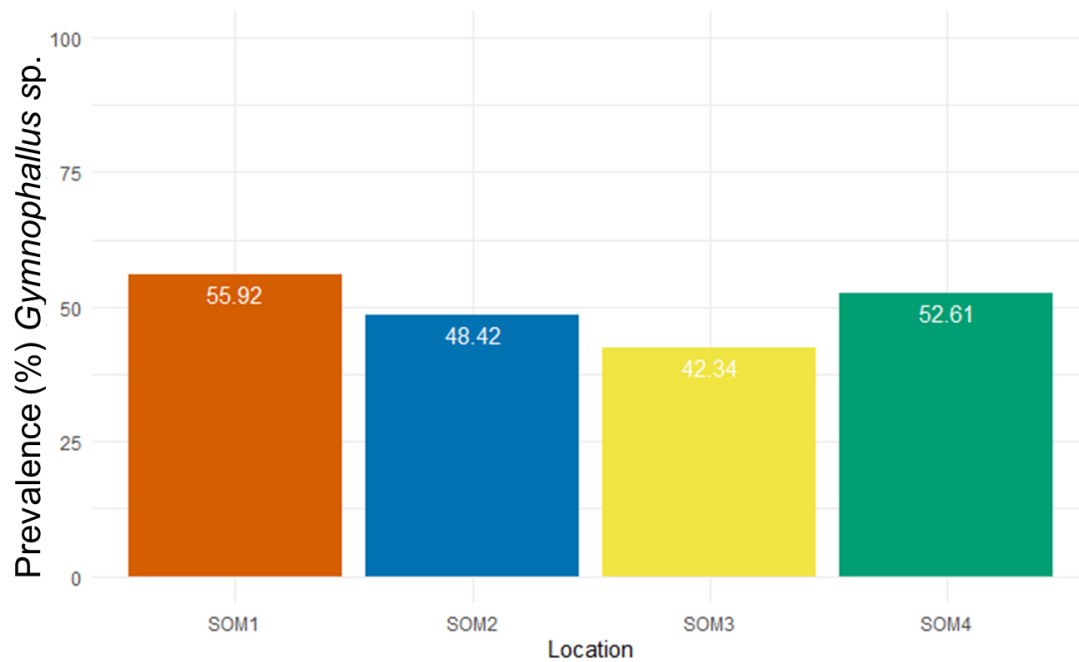


Figure 14 - Prevalence of *Gymnophallus* sp. at each location locations (SOM1 orange, SOM2 blue, SOM3 yellow, SOM4 green) in percentages (%), averaged over seasons. Data are displayed in a bar chart with prevalence in percentages indicated in white.

Table 7 - Comparisons based on a generalized linear model showing differences in infection likelihood of *Gymnophallus* sp. between sampling locations and seasons. The table displays a combination of different outputs from the same model, obtained by releveling the factors. Values given are (from left to right): model estimate; standard error, z-value, and p-value. Statistically significant results where $p \geq 0.05$ are indicated in bold.

| glm(Gymnophallus_sp._Bin ~ (Location+Season+Length+Location*Season),family = binomial(link = "logit"),data) | | | | |
|--|--------------|-------------|--------------|--------------|
| i.Location - Location | Estimate | Std. Error | z value | Pr(> z) |
| SOM1 - SOM2 | -0.31 | 0.13 | -2.45 | 0.014 |
| SOM1 - SOM3 | -0.51 | 0.16 | -3.11 | 0.002 |
| SOM1 - SOM4 | -0.11 | 0.16 | -0.66 | 0.512 |
| SOM2 - SOM3 | -0.19 | 0.16 | -1.22 | 0.222 |
| SOM2 - SOM4 | 0.21 | 0.16 | 1.31 | 0.191 |
| SOM3 - SOM4 | 0.40 | 0.17 | 2.34 | 0.019 |
| ii.Season - Season | | | | |
| fall - spring | -0.15 | 0.15 | -1.02 | 0.308 |
| fall - summer | -0.39 | 0.16 | -2.37 | 0.018 |
| fall - winter | -0.03 | 0.14 | -0.18 | 0.860 |
| winter - spring | -0.12 | 0.16 | -0.80 | 0.426 |
| winter - summer | -0.36 | 0.16 | -2.22 | 0.026 |
| spring - summer | -0.24 | 0.16 | -1.49 | 0.137 |

Effects of wave exposure - Wave exposure did not affect the infection likelihood with *Gymnophallus* sp. (Appendix 32). When analyzing the infection likelihood with *Gymnophallus* sp. by including the interactive effects of location and wave exposure as well as season and wave exposure, some location and season-specific differences became apparent (Appendix 33, 34).

Effect of intertidal level - Along the intertidal gradient, some levels displayed differences in infection likelihood with *Gymnophallus* sp. (Figure 13, Appendix 35). Intertidal level ‘low’ had a lower infection likelihood than level ‘high’ (Appendix 35). When the interaction effects of season and intertidal level, as well as location and intertidal level, were included in the analysis on effects on infection likelihood with *Gymnophallus* sp., some location and level-specific differences became apparent, however, no general pattern was displayed along the intertidal gradient (Appendix 36, 37).

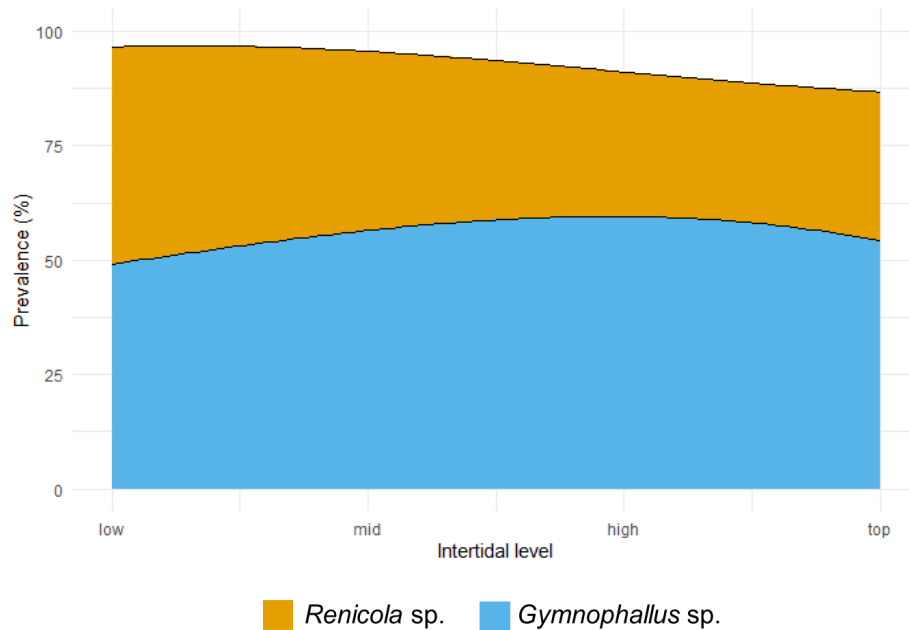


Figure 13 - Prevalence of *Renicola* sp. (orange) and *Gymnophallus* sp. (blue) along the intertidal gradient at both natural sites combined. In general, we can observe that the prevalence of *Renicola* sp. decreases with increasing intertidal levels, and the prevalence of *Gymnophallus* sp. peaks at level ‘high’.

Summary of infection patterns in *Renicola* sp. and *Gymnophallus* sp. - In summary, patterns in infection intensity and prevalence of *Renicola* sp. were expressed to a greater extent, where natural locations had a higher infection intensity and prevalence than human-influenced sites. The infection intensity of *Renicola* sp. increased during fall. Blue mussels at wave-sheltered sites harbored a greater number of *Renicola* sp. than the wave-exposed sites and a greater infection intensity and prevalence of *Renicola* sp. was found at the lower levels along the intertidal zone. *Gymnophallus* sp. had generally less expressed patterns between the different locations but showed a higher infection intensity and prevalence at SOM1 and SOM4 compared to SOM2 and SOM3. During summer, infection intensity and prevalence of *Gymnophallus* sp. was at its lowest. Wave exposure and intertidal level did not influence the abundance of *Gymnophallus* sp., with the exemption of infection intensity and prevalence at intertidal level ‘high’.

3.2. Additional Biodiversity Data

The composition of bird functional groups was relatively comparable at all four locations. However, SOM3 showed a greater abundance of waders compared to the other sites, and proportionally fewer gulls (Figure 14). All birds and functional groups mentioned in the literature were found in the Sommarøy area, which confirms possible infection at all sites.

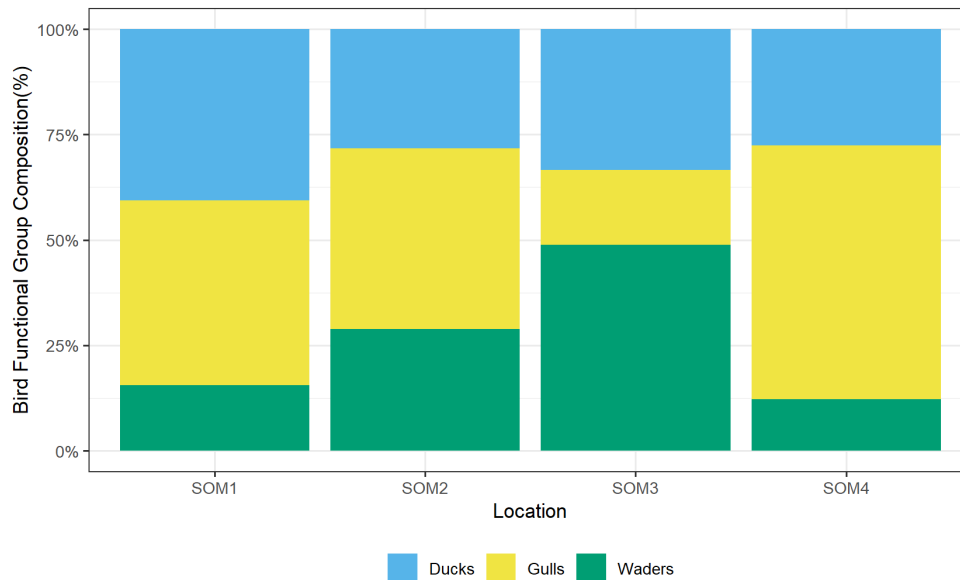


Figure 14 - Bird functional composition at Sommarøya area. The graph shows the proportional distribution of Ducks, Gulls, and Waders in the Sommarøy area at each sampling location. Data retrieved from *Artskart (2024)*.

The algae and lichen species richness among the different sites differs especially between natural and human-influenced locations, with higher species richness at natural locations (Table 7). Field observations showed a dominance of red algae at SOM1E and SOM2E while SOM1S and SOM2S displayed heterogeneous and diverse communities with algae and lichen. At all sites with natural substrate, a coverage of vegetation was found after visual inspection compared to SOM4E, SOM4S, and SOM3E. Human-constructed sites SOM4E and SOM4S, and SOM3E displayed less biomass abundance and were mostly dominated by *Ascophyllum nodosum* and *Fucus spiralis*.

Table 7 - Table showing the algae and lichens species richness at all sampling sites in the Sommarøy area. The number of brown, red, and green algae and lichens was assessed and compared between sites.

| | SOM1E | SOM1S | SOM2E | SOM2S | SOM3e | SOM3s | SOM4E | SOM4S |
|-----------|-------|-------|-------|-------|-------|-------|-------|-------|
| Brown | 7 | 9 | 8 | 8 | 6 | 7 | 7 | 6 |
| Red algae | 4 | 5 | 6 | 6 | 3 | 4 | 1 | 1 |
| Green | 3 | 1 | 2 | 2 | 2 | 2 | 1 | 2 |
| Lichens | 0 | 1 | 1 | 1 | 0 | 0 | 1 | 1 |
| all | 14 | 15 | 17 | 17 | 11 | 11 | 10 | 10 |

Gastropod density was highest at SOM3 and SOM4, the two human-influenced locations (Table 8, Appendix 38). This pattern stands contrary to a higher observed infection intensity and prevalence of *Renicola* sp. at natural sites and does not correspond to a higher infection intensity and prevalence of *Gymnophallus* sp. at SOM1 and SOM4.

Table 8 - Total gastropods (*Littorina obtusata*, *Nucella lapillus*, *Littorina saxatilis*, and *Littorina littorea*) observations at each site throughout all seasons (winter, spring, summer, and fall) sampled in a 50*50 square.

| | SOM1E | SOM1S | SOM2E | SOM2S | SOM3E | SOM3S | SOM4E | SOM4S |
|---------|-------|-------|-------|-------|-------|-------|-------|-------|
| winter | 4 | 16 | 0 | 9 | 2.5 | 19 | 10 | 2 |
| spring | 6 | 28.5 | 0 | 8.5 | 47 | 65.5 | 24.5 | 14 |
| summer | 55 | 24 | 16 | 13.5 | 35.5 | 203 | 47 | 46 |
| fall | 4 | 9 | 5.5 | 10.5 | 108 | 98.5 | 15 | 45.5 |
| average | 17.25 | 19.38 | 5.38 | 10.3 | 69.5 | 96.38 | 24.13 | 26.88 |

*Numbers are the average count of 2 50*50 sample frames

4. Discussion

Blue mussels play an important role in the intertidal zone and are hosts to various trematode species, affecting their functioning in the intertidal ecosystem (e.g. Gosling, 2008; Wilson et al., 2013, Hilgerloh, 1997). The present study highlights that trematode community structure and infection rates in blue mussels in Arctic Norway show species-specific differences on various spatial scales and with seasonality. Three trematode species were found, all of which were identified to the genus level. Opposing my first hypothesis, where higher trematode abundance at human-influenced locations was expected, *Renicola* sp. showed a greater infection intensity and prevalence at natural locations while *Gymnophallus* sp. showed no significant difference between natural and human-influenced locations. My second hypothesis, where higher infection intensity and prevalence at sheltered sites compared to wave-exposed sites were suspected, was confirmed for *Renicola* sp. but can be rejected for *Gymnophallus* sp.. Similarly, patterns were found in the distribution along the intertidal gradient for *Renicola* sp. but not for *Gymnophallus*, confirming my third hypothesis for *Renicola* sp. only. Finally, my fourth hypothesis, the effect of seasonality on both species' infection intensity and prevalence, cannot be confirmed.

When comparing species throughout the seasons, it is important to consider their species-specific life cycles. In the case of *Renicola* sp., the complex life cycle involves cercariae released from sporocysts within gastropods, which then encyst as metacercariae in bivalves like blue mussels. This is followed by trophic transmissions to their final hosts, such as waders or gulls (Werding, 1969). As both intermediate and final hosts are present in the area throughout the year, new infections could, in theory, occur independent of seasonality (Fonstad et al., 2008). However, *Renicola* sp. most likely transmits via its free-living stage during the warmer seasons, as higher infection intensity was found in the fall, after the vegetative period. Previous studies support this assumption of a transmission peak during the summer season (Combes et al., 1994; Thieltges & Rick, 2006; Werding, 1969). For instance, cercaria of *Renicola* spp. use temperature and phototaxis as indications for emergence, as cercariae were found to emerge at 10-15°C, and a strong correlation with cercariae emergence during the highest daily temperature has been reported (Prokofiev et al., 2016). The changes in infection intensity and prevalence were surprisingly low when comparing different seasons. It is possible that *Renicola* sp. can accumulate throughout a mussel's lifetime, as infections during the Arctic winter are unlikely (Galaktionov et al., 2006; Lauckner, 1983). This could explain why the seasonal differences were subtle and are supported by literature suggesting trematodes' lifespan

is limited by that of their hosts only (Galaktionov et al., 2006). However, the emergence and winter survival of cold-adapted Arctic parasite populations should be assessed in future research (see also Selbach et al., 2024).

In contrast, the life cycle of *Gymnophallus* sp. has been studied to a lesser extent. Like *Renicola* spp., gymnophalloids use gastropods or molluscs as their first intermediate host, where cercariae are emitted from sporocysts and then form unencysted metacercaria within gastropods or molluscs. Their life cycle is completed after transmission to wading birds or diving ducks (Benito et al., 2022; Chung et al., 2010; Cremonte et al., 2015; Ryang et al., 2000; Szidat, 1962). However, variations of the life cycle have been described, leaving some doubt about the exact hosts and life history traits of the parasite (Cable, 1953; Cremonte, 2015; Lauckner, 1983; Loos-Franck, 1969; Szidat, 1962). For example, while the trematode undergoes the process of calcification, pearls and mucus envelopes cannot always be identified clearly as gymnophalloids, even though literature suggests this to be the case (e.g. Benito et al., 2023; Lauckner, 1983). This complex and understudied life cycle as well as morphological variation could explain why distribution patterns were unclear for *Gymnophallus* sp. Life cycle strategies used by Arctic gymnophalloids have not been studied experimentally and would be of great interest for further research, as stressors and environmental conditions in these regions are unique.

Considering that the life cycles of gymnophalloids are not completely explored, interpretation of seasonal effects is only possible to a limited extent. Survival throughout several years is suggested for *Gymnophallus* spp. in the literature, similar to *Renicola* sp. (Lauckner, 1983; Loos-Frank, 1969). As the peak in infection intensity and infection prevalence differed between species, one could interpret species-specific timing of cercarial emission and transmission for both species. This study focused on one part of the trematodes' lifecycle, the metacercarial stage within their second intermediate host. However, distribution and abundance are likewise influenced by the parasites' first intermediate host and their final bird hosts, which will need to be identified to better explain the observed patterns.

Intermediate and final host abundance and heterogeneity have been identified as drivers of trematode abundance (e.g. Hechinger & Lafferty, 2005). In previous findings, the high abundance of trematodes around fish farms and fish factories in northern Norway was linked to high bird presence, specifically gulls (Byers et al., 2008; Galaktionov, 2015; Werding, 1969). This effect was not observed at my sample locations, where a higher proportion of gulls could

not be linked to proximity to human-influenced locations or locations with high trematode abundance. Timing of fishery activities and gull presence could be investigated in relation to trematode transmission for possible explanations. A higher abundance of *Gymnophallus* sp. at individual locations (SOM4) seemed to coincide with a higher proportion of gulls, however, gulls are not commonly described as final hosts for gymnophalloids. More research on host specificity of *Gymnophallus* sp. and *Renicola* sp. in Arctic habitats is needed to understand and link possible effects of final hosts and their abundance.

In addition to bird abundance, gastropod presence has been identified as one of the main drivers of parasite abundance (e.g. Bustnes & Galaktionov, 1999; Wilson et al., 2013). This is assumed, as mussels acquire their trematode infections from the transmission stages released from gastropod intermediate hosts. A greater abundance of gastropods at human-influenced locations was found compared to natural locations. Additionally, wave-sheltered sites showed a higher abundance of gastropods than wave-exposed sites. As trematode infection intensity and prevalence show inconclusive trends in snail abundance when comparing locations, my findings contradict the assumption that greater parasite prevalence in mussels is, by definition, linked to the greater abundance of snails. It is, however, possible, that snails retreated in the subtidal zone during low tide to avoid predation, desiccation, and wave exposure at exposed natural locations. An alternative measuring method to take the mobility of the gastropods into account would be useful when assessing snail abundance in the future. Nonetheless, snail abundance alone did not explain trematode prevalence and infection intensity, leading to the assumption that local variation in infection prevalence or cercarial productivity within snails could be a better indicator for parasite presence in blue mussel populations and should be assessed in Arctic region (Fernandez & Esch, 1991).

While bird and snail abundance did not offer a full explanation for trematode distribution along the locations, overall species richness of algae and lichens did to a higher degree. At sites with higher infection intensity and prevalence of *Renicola* sp., a greater species richness of algae and lichens was observed. The data suggests that species richness impacts blue mussels and trematodes directly or indirectly, by providing a more heterogeneous habitat for blue mussels or other hosts. Vegetation-rich patches likely provide shelter or favourable feeding conditions for molluscs and birds, potentially enhancing trematode transmission and creating infection hotspots at the sampling sites. This finding is surprising, as it contradicts previous assumptions, where macroalgae were found to have negative effects on cercarial transmission (Prinz et al.,

2009; Welsh et al., 2014). In addition, registration of sessile vegetation at sample sites does not pose the same difficulties in reporting as for mobile species such as gastropods and birds and might therefore be a better indicator for trematode abundance. Conversely, parasites can be an indicator of more stable and healthy ecosystems (Hechinger & Lafferty, 2005; Landsberg et al., 1998; Loot et al., 2005; Marcogliese, 2005; Moor et al., 2020). It can therefore be concluded that biotic factors, which differ between location and sites directly or indirectly influence parasite communities in the intertidal zone. These biotic factors are influenced by abiotic factors, which shape the environment in which these communities are found.

Wave exposure was assessed as an abiotic stressor, which affects cercariae during transmission periods as well as reducing blue mussel's ability to attach to substrate (Babarro & Carrington, 2013; Granovitch & Mikhailova, 2004). In this study, a greater infection rate of *Renicola* sp. was observed at wave-sheltered sites, but no difference was apparent for *Gymnophallus* sp. At sheltered sites and in the intertidal pools sheltered by rock and vegetation, a greater number of canopy-building algae (e.g. *Ascophyllum nodosum*) was present, sheltering the mussels from quick water exchange and wave exposure and thus effectively altering abiotic conditions, potentially facilitating habitat. The idea, that facilitation becomes increasingly significant in harsh or extreme environments is addressed by the Stress Gradient Hypothesis (SGH) and might explain why this positive effect through macroalgae has not been observed in lower latitude studies (Bertness and Callaway, 1994; Bertness et al., 1999; Holmgren and Scheffer, 2010; Stachowicz, 2001). These algae might provide a direct advantage for trematodes by reducing water turbulence, leading to easier transmission between hosts at locations where extreme wave exposure would otherwise be a disruptive factor. Moreover, these protected and shallow waters will likely allow warmer water temperatures during sunshine, and thereby facilitate parasite transmission in these microhabitats.

These patterns highlight the difficulty of distinguishing between biotic and abiotic impacts on trematode communities in field experiments. The complex interplay of various variables affecting cercarial transmission makes it difficult to identify singular drivers. Human-influenced sites, for example, had a lower prevalence and infection intensity even though locations were protected from the direct wave exposure of open Atlantic water. It is probable, that the generally more sheltered condition at human-influenced sites did not provide the same advantage as the natural tidal pools for trematodes, because these were overshadowed by negative human influences, such as lack of natural conditions or pollution (Lafferty, 1997; Thieltges et al., 2008; Moore et al., 2020). Thus, the possible additive or antagonistic effects of

biotic and abiotic drivers need to be considered and investigated in greater detail. Here, controlled laboratory or mesocosm experiments could help to decipher the contribution of each variable as well as their potential interactive effects.

Differences in trematode communities between sites were however also observed at human-influenced locations. Prevalence of *Renicola* sp. and *Gymnophallus* sp. differed up to 11.7 % and 10.7 %, respectively with just a few meters distance between sites at a human-influenced location (SOM3). These differences could not be attributed to obvious external factors, as the conditions (wave exposure, substrate, and vegetation) were very similar at both sites. Here, again, local variation of prevalence in upstream hosts could explain differences (see above). Bird abundance can likely be a driver for trematode infection rates at a larger scale, while site-specific conditions locally influence trematode prevalence and infection intensity (Byers et al., 2008; Fredensborg et al., 2006). This point of view is also supported by bulk emissions strategies of the trematodes from their first hosts, which could lead to locally high infection variations at small scales (Combes et al., 1994). To gain conclusive insight into how certain variables, human influence, in this case, affect infection rates, an increase in sampling sites would be useful for future studies, not at last to increase statistical power.

Differences at an even smaller scale, along the intertidal gradient, could be driven by hosts' and parasites' behavioural adaptations. Here, *Renicola* sp. was more abundant at lower levels in the intertidal zone. A host-specific distribution of trematodes along the intertidal levels was expected, with higher infections with *Renicola* sp. 'top' levels, as seagulls feed close to the surface. *Gymnophallus* sp., on the other hand, were predicted to be more abundant at lower levels, as they complete their life cycle in diving ducks (Galaktionov & Bustnes, 1996). However, such a pattern could not be observed in the present study. Lower infection intensity with *Renicola* sp. at higher intertidal levels could be caused by predation pressures and stress-induced reduced fitness (e.g. desiccation, freezing), which could lead to a die-off of heavily infected mussels (Widdows & Shick, 1985). Thieltges (2006) identified metacercariae as a constant stressor in blue mussels, and Selbach et al. (2024) reported trematode-induced mortality in mussels during the winter. The interactive effects of parasites with desiccation, predation, and extreme temperatures could thus reduce mussels' fitness, as energy expenditure is a trade-off between mussel growth, reproduction, and defence against parasites.

It was hypothesized that infection intensity and prevalence would be greater at higher intertidal levels. This trend was, however, not observed, possibly due to negative effects of trematodes

which in addition to abiotic factors and predation could have had lethal effects for mussels at these higher intertidal levels. If this were true, higher infection intensity and prevalence of *Renicola* sp. at 'top' levels during fall, when newly heavily infected mussels have not yet died, would be expected. This was not the case in the present study. Therefore, other explanations for greater infection intensity and prevalence of *Renicola* sp. at lower intertidal levels should be considered. Accumulation of *Renicola* sp. at subtidal and littoral levels has been found in other studies as well (e.g. Nikolaev, 2017; Thieltges, 2006; Thieltges, 2007). Continuous mussel feeding and filtration at lower intertidal levels leads to a higher likelihood of cercarial ingestions. Additionally, it was suggested that other factors such as high, unregulated emission of cercariae by their first host, water turbulence, tidal level at the timing of emissions, and ingestion by chance could overshadow expected patterns in addition to stress and predation-related die-offs (Thieltges, 2006). These factors might also play a role in the present samples. Altogether, this highlights the need for small scale and manipulative studies in trematode distribution along the intertidal gradient.

However, intertidal stress is not the only possible explanation for variation in trematode abundance. Location-, site-, and tidal level-specific variation in blue mussel physiology, adaptation, immunity, growth patterns, and filtration are possible determinants of parasite infection (e.g. Christensen et al., 2015; Mair et al., 2007; Shields et al., 2008; Place et al., 2008; Shick et al., 1986; Tolman et al., 2019). For instance, species-specific tolerance and immunity of *M. edulis*, *M. trossulus*, *M. galloprovincialis*, and hybrids to trematodes could explain differences between locations. Certain trematodes have been found to castrate *M. edulis* while *M. galloprovincialis* (which are invasive to Norway) are not affected by these parasites (Coustau et al., 1991; Lise et al., 2018; Marchioro et al., 2023). Such species-specific susceptibility could also be true for *Renicola* sp. and *Gymnophallus* sp. Future studies should therefore further investigate susceptibility to trematode infections between species of the genus *Mytilus*. In addition to its parasitological importance, these differences are important for a better understanding of invasive species, hybridization, and northwards expansions of historically southern species, and their effects on Arctic coastal ecosystems (Berge et al., 2005).

Intraspecific variation between mussels, e.g., age and length of the mussels, could possibly explain trematode accumulation patterns. Such patterns have been found in other studies, where abundance was higher within larger mussels (e.g. Bommarito et al., 2021). However, location or site-specific growth rates and infection patterns make comparison of length between location, sites, and intertidal level difficult (Sellæg, 2023). Additionally, a reduced growth rate with

higher infection makes mussel length a problematic indicator for trematode infection (Thieltges, 2006). Moreover, recent studies have shown that even low levels of trematode infections can impair the growth of blue mussels under cold conditions (Selbach et al., 2024). Long-term, observations of experimentally infected blue mussels or including mussel age as a variable would help to understand possible accumulation and trematode abundance at a deeper level.

Additionally, location- and site-specific trematode accumulation could be influenced by mussel filtration rate, as exposure to cercariae increases with increasing mussel filtration rate. (Liddell et al., 2017). If mussels at natural locations have significantly higher filtration rates, as more effort is needed to ingest the same amount of food compared to eutrophic human-influenced locations, they would respectively have a higher chance of ingesting cercariae. It is, however, unlikely that differences in filtration rate are due to nutrient availability, as saturation and accompanied reduction of filtration are rarely found in situ (Clausen & Riisgrd, 1996; Maire et al., 2007). Instead, a minimum of nutrients is required to trigger filtration, while in the absence of food, mussels' valves stay closed (Dolmer, 2000; Luskow et al., 2018). Nutrient availability and possible correlation with trematode accumulation due to higher filtration rates could be a topic for future studies, especially regarding expected increases in primary production, climate change, and global warming (Maar et al., 2024; Kamermans & Saurel, 2022).

When comparing my findings from the Sommarøya area to those of previous studies from Arctic mussel populations, the species composition appears similar, as both *Renicola* sp. and *Gymnophallus* sp. were found in previous studies as well. *Himasthla* sp. was only found in two of my sample mussels, in stark contrast to the higher prevalence reported by Galakinionov et al. (2015) and Benito et al. (2022). This discrepancy could possibly be attributed to species-specific habitat requirements, as miracidia of *Himasthla* sp. develop over an extended period of 10 days to up to four weeks, requiring higher temperatures (15-20°C) for ripening and hatching, as commonly observed in low tide mudflat areas (Loos-Frank, 1967; Stunkard, 1938; 1960; Werding, 1969). Additionally, *Himasthla* species tend to appear later during the vegetative season (Loos-Frank, 1967). The absence of sandy intertidal areas at the sampling sites in the present study, combined with the timing of the sampling, could explain the low abundance of *Himasthla* sp. compared to the other trematode species in this study.

Prevalence rates of trematodes across locations in the Sommarøy area, as examined in this study, show variation compared to sites studied previously around Tromsø city (Appendix 39). Benito et al. (2022) and Galaktionov et al. (2015) observed similar trends, noting higher trematode accumulation in more natural locations. However, the unclear distinction between natural and human-influenced sites in these earlier studies makes direct comparisons inconclusive. Additionally, no latitudinal gradient in trematode prevalence is apparent when comparing all three studies. As discussed by Thielges et al. (2009), spatial heterogeneity at smaller scales may overshadow large-scale patterns in trematode distribution, as no trend is apparent along the Norwegian coast, as supported by other studies (Byers et al., 2008; Hechinger & Lafferty, 2005; Fredensborg et al., 2006; Poulin & Leung, 2011; Struder et al., 2013, Thielges et al., 2009). It can be noted, however, that prevalence levels in my study region were amongst the highest reported for these two trematode species, indicating favorable conditions for these parasites in northern Norway.

Regardless of the exact drivers and mechanisms of the observed infection patterns in Arctic *Mytilus* populations, trematode infections likely have significant implications for both their hosts and the coastal ecosystem. *Renicola* sp., here found in high infection intensity, for example, has been shown to reduce filtration and growth rates in *Mytilus* (Stier et al., 2015; Thielges et al., 2006, 2022). Present in lower infection intensity, metacercariae of gymnophalloids seem to actively feed on host tissue and have been reported to negatively affect fecundity and survival in other mollusks (de Montaudouin et al., 2021; Lauckner, 1971). This feeding behavior may explain why blue mussels invest in costly calcification around *Gymnophallus* sp. and not the other trematodes (*Renicola* sp. in our case) (de Montaudouin et al., 2021; Marchiori et al., 2023; Lauckner, 1971). If Gymnophalloids trigger defense mechanisms in their hosts due to their active predation, they could potentially have a great impact on intertidal ecosystems, despite their relatively low prevalence and infection intensity.

To conclude, differences in parasite communities can be found within several hundred meters, between wave-exposed and wave-sheltered microhabitats with just a few meters distance, and between the different levels of the intertidal zone. These variations are influenced, at least in part, by the four key factors discussed and analyzed in this thesis. Human activities impact biotic environments (e.g. vegetation cover and host distribution) and abiotic conditions (e.g. substrate, and nutrient or toxin release), which were found to negatively affect *Renicola* sp. infection rates either directly or indirectly. Wave exposure, an abiotic factor, was associated with reduced *Renicola* sp. infection intensity and infection prevalence at the surveyed sites,

whereas biotic interactions, such as facilitation by macroalgae, may have created favorable conditions for *Renicola* sp.. Behavioral adaptations of cercariae did not appear to lead to expected patterns, i.e., distribution according to preferred final hosts of the trematode species and yet, other factors might influence cercarial distribution patterns along the intertidal gradient (e.g. highest survival rate). There seemed to be some seasonal change, especially with an increase in infection intensity for *Renicola* sp. after the vegetative period (fall). However, while four selected factors possibly influencing trematode distribution were analyzed, one must be aware of the interactive, additive, synergistic, or antagonistic effects ways all these factors influencing each other and the parasite-host relationship.

My findings underscore that a holistic and multidimensional approach is required when assessing trematode abundance in blue mussels, emphasizing the significance of temporal-spatial considerations. While it is broadly held that trematodes play a key role in intertidal food webs, their exact interactions and dependencies within the wider ecosystem are not yet fully understood. Their role in the Arctic intertidal system is important to understand and future research will help to further decode these complex interactions blue mussels with their abundant and unique trematode communities, present a valuable and fascinating opportunity to investigate these interspecific relationships in Arctic regions.

5. References

- Artskart.artsdatabanken.no (2024). Downloadet from 'Artskart'. Accessed: 13.04.2024. <https://artskart.artsdatabanken.no>
- Babarro, J. M., & Carrington, E. (2013). Attachment strength of the mussel *Mytilus galloprovincialis*: effect of habitat and body size. *Journal of Experimental Marine Biology and Ecology*, *443*, 188-196. <http://doi.org/10.1016/j.jembe.2013.02.035>
- Benito, D., Izagirre, U., Lekube, X., Zaldibar, B., Villalba, A., de Montaudouin, X., Daffe, G., Soto, M., & Diaz De Cerio, O. (2023). Molecular confirmation of pearl formation in arctic mussels (*Mytilus edulis*) caused by *Gymnophallus bursicola* (Odhner 1900) metacercariae. *Parasitology*, *150*(11), 1015–1021. <https://doi.org/10.1017/S0031182023000860>
- Benito, D., Paleček, D., Lekube, X., Izagirre, U., Marigómez, I., Zaldibar, B., & Soto, M. (2022). Variability and distribution of parasites, pathologies and their effect on wild mussels (*Mytilus* sp.) in different environments along a wide latitudinal span in the Northern Atlantic and Arctic Oceans. *Marine Environmental Research*, *176*, 105585. <https://doi.org/10.1016/j.marenvres.2022.105585>
- Berge, J., Johnsen, G., Nilsen, F., Gulliksen, B., & Slagstad, D. (2005). Ocean temperature oscillations enable reappearance of blue mussels *Mytilus edulis* in Svalbard after a 1000 year absence. *Marine Ecology Progress Series*, *303*, 167-175. <https://doi:10.3354/meps303167>
- Bertness, M. D., & Callaway, R. (1994). Positive interactions in communities. *Trends in ecology & evolution*, *9*(5), 191-193. [https://doi.org/10.1016/0169-5347\(94\)90088-4](https://doi.org/10.1016/0169-5347(94)90088-4)
- Bertness, M. D., Leonard, G. H., Levine, J. M., Schmidt, P. R., & Ingraham, A. O. (1999). Testing the relative contribution of positive and negative interactions in rocky intertidal communities. *Ecology*, *80*(8), 2711-2726. [https://doi.org/10.1890/0012-9658\(1999\)080\[2711:TTRCOP\]2.0.CO;2](https://doi.org/10.1890/0012-9658(1999)080[2711:TTRCOP]2.0.CO;2)
- Bommarito, C., Thieltges, D. W., Pansch, C., Barboza, F. R., Pranovi, F., Wahl, M. (2021). Effects of first intermediate host density, host size and salinity on trematode infections in mussels of the south-western Baltic Sea. *Parasitology*, *148*(4), 486–494. <https://doi.org/10.1017/S0031182020002188>
- Bouallegui, Y. (2019). Immunity in mussels: An overview of molecular components and mechanisms with a focus on the functional defenses. *Fish and Shellfish Immunology*, *89*, 158-169. <https://doi.org/10.1016/j.fsi.2019.03.057>
- Bracken, M. E., Menge, B. A., Foley, M. M., Sorte, C. J., Lubchenco, J., & Schiel, D. R. (2012). Mussel selectivity for high-quality food drives carbon inputs into open-coast intertidal ecosystems. *Marine Ecology Progress Series*, *459*, 53-62. <https://doi.org/10.3354/meps09764>
- Brenner, M., Broeg, K., Frickenhaus, S., Buck, B. H., & Koehler, A. (2014). Multi-biomarker approach using the blue mussel (*Mytilus edulis* L.) to assess the quality of marine

- environments: season and habitat-related impacts. *Marine environmental research*, 95, 13-27. <https://doi.org/10.1016/j.marenvres.2013.12.009>
- Brooks, S. J., & Farnen, E. (2013). The distribution of the mussel *Mytilus* species along the Norwegian coast. *Journal of Shellfish Research*, 32(2), 265-270. <https://doi.org/10.1016/j.fsi.2019.03.057>
- Buck, B. H., Thieltges, D. W., Walter, U., Nehls, G., & Rosenthal, H. (2005). Inshore–offshore comparison of parasite infestation in *Mytilus edulis*: implications for open ocean aquaculture. *Journal of applied ichthyology*, 21(2), 107-113. <https://doi.org/10.1111/j.1439-0426.2004.00638.x>
- Buck, J. C. (2019). Indirect effects explain the role of parasites in ecosystems. *Trends in Parasitology*, 35(10), 835-847. <https://doi.org/10.1016/j.pt.2019.07.007>
- Bush, A. O., Lafferty, K. D., Lotz, J. M., & Shostak, A. W. (1997). Parasitology meets ecology on its own terms: Margolis et al. revisited. *The Journal of parasitology*, 83(4), 575-583. <https://doi.org/10.2307/3284227>
- Bustnes, J. O., & Erikstad, K. E. (1988). The diets of sympatric wintering populations of common eider *Somateria mollissima* and king eider *S. spectabilis* in northern Norway. *Ornis Fennica*, 65(4), 163-168. <https://ornisfennica.journal.fi/article/view/133269>
- Bustnes, J. O., & Galaktionov, K. (1999). Anthropogenic influences on the infestation of intertidal gastropods by seabird trematode larvae on the southern Barents Sea coast. *Marine Biology*, 133, 449-453. <https://doi.org/10.1007/s002270050484>
- Byers, J. E., Blakeslee, A. M., Linder, E., Cooper, A. B., & Maguire, T. J. (2008). Controls of spatial variation in the prevalence of trematode parasites infecting a marine snail. *Ecology*, 89(2), 439-451. <https://doi.org/10.1890/06-1036.1>
- Cable, R.M., 1953. The life cycle of *Parvatrema borinquenae* gen. et sp.nov. (Trematoda: Digenea) and the systematic position of the subfamily Gymnophallinae. *Journal of Parasitology* 39: 408-421. <https://doi.org/10.2307/3274284>
- Christensen, H. T., Dolmer, P., Hansen, B. W., Holmer, M., Kristensen, L. D., Poulsen, L. K., ... & Støttrup, J. G. (2015). Aggregation and attachment responses of blue mussels, *Mytilus edulis* - impact of substrate composition, time scale and source of mussel seed. *Aquaculture*, 435, 245-251. <https://doi.org/10.1016/j.aquaculture.2014.09.043>
- Chung, O. S., Lee, H. J., Sohn, W. M., Park, Y. K., Chai, J. Y., & Seo, M. (2010). Discovery of *Parvatrema duboisi* and *Parvatrema homoeotecnum* (Digenea: Gymnophallidae) from migratory birds in Korea. *The Korean Journal of Parasitology*, 48(3), 271-274. <https://doi:10.3347/kjp.2010.48.3.271>
- Clausen, I., & Riisgård, H. U. (1996). Growth, filtration and respiration in the mussel *Mytilus edulis*: no evidence for physiological regulation of the filter-pump to nutritional needs. In *Marine Ecology Progress Series*, 141(1-3), 37-45. <https://doi:10.3354/meps141037>

- Combes, C., Fournier, A., Mone, H., & Theron, A. (1994). Behaviours in trematode cercariae that enhance parasite transmission: Patterns and processes. *Parasitology*, 109 Suppl(S1):S3-13. <https://doi.org/10.1017/s0031182000085048>
- Cornelius, A., Buschbaum, C., Khosravi, M., Waser, A. M., Wegner, K. M., & Thieltges, D. W. (2023). Effect of predation risk on parasite transmission from first to second intermediate trematode hosts. *Journal of Animal Ecology*, 92(5), 991-1000. <https://doi.org/10.1111/1365-2656.13921>
- Coustau, C., Renaud, F., Maillard, C., Pasteur, N., & Delay, B. (1991). Differential susceptibility to a trematode parasite among genotypes of the *Mytilus edulis/galloprovincialis* complex. *Genetics Research*, 57(3), 207-212. <https://doi.org/10.1017/s0016672300029359>.
- Cremonte, F., Gilardoni, C., Pina, S., Rodrigues, P., & Ituarte, C. (2015). Revision of the family Gymnophallidae Odhner, 1905 (Digenea) based on morphological and molecular data. *Parasitology International*, 64(2), 202–210. <https://doi.org/10.1016/j.parint.2014.12.003>
- de Montaudouin, X., Arzul, I., Cao, A., Carballal, M. J., Chollet, B., Correira, S., ... & Villalba, A. (2021). Catalogue of parasites and diseases of the common cockle *Cerastoderma edule*. <https://doi.org/10.34624/9a9c-9j21>
- Dunne, J. A., Lafferty, K. D., Dobson, A. P., Hechinger, R. F., Kuris, A. M., Martinez, N. D., ... & Zander, C. D. (2013). Parasites affect food web structure primarily through increased diversity and complexity. *PLoS biology*, 11(6), <https://doi.org/10.1371/journal.pbio.1001579>
- Eggermont, M., Cornillie, P., Dierick, M., Adriaens, D., Nevejan, N., Bossier, P., ... & Declercq, A. M. (2020). The blue mussel inside: 3D visualization and description of the vascular-related anatomy of *Mytilus edulis* to unravel hemolymph extraction. *Scientific reports*, 10(1), 6773. <https://doi.org/10.1038/s41598-020-62933-9>
- Espinasse, M., Mikkelsen, E., Sørbye, S. H., Skern-Mauritzen, M., Falk-Andersson, J., & Fauchald, P. (2023). Seafood production in Northern Norway: Analyzing variation and co-development in aquaculture and coastal fisheries. *Marine Policy*, 155, 105777. <https://doi.org/10.1016/j.marpol.2023.105777>
- Fernandez, J., & Esch, G. W. (1991). Guild structure of larval trematodes in the snail *Helisoma anceps*: patterns and processes at the individual host level. *The Journal of parasitology*, 528-539. <https://doi.org/10.2307/3283157>
- Fingerut, J. T., Zimmer, C. A., & Zimmer, R. K. (2003). Larval swimming overpowers turbulent mixing and facilitates transmission of a marine parasite. *Ecology*, 84(9), 2502–2515. <https://doi.org/10.1890/02-4035>
- Fonstad, T., Génsbøl, B., Günther, M., Andersen, J. F., & Bertel, B. (2008). *Aschehougs fuglebok med CD-er*. Oslo: Aschehoug. ISBN 978-82-03-23569-6.
- Fredensborg, B. L., Mouritsen, K. N., & Poulin, R. (2006). Relating bird host distribution and spatial heterogeneity in trematode infections in an intertidal snail—from small to large scale. *Marine Biology*, 149, 275-283. <https://doi.org/10.1007/s00227-005-0184-1>

- Galaktionov, K. V., & Bustnes, J. O. (1999). Distribution patterns of marine bird digenean larvae in periwinkles along the southern coast of the Barents Sea. *Diseases of aquatic organisms*, 37(3), 221-230. <https://doi.org/10.3354/dao037221>
- Galaktionov, K. V., Bustnes, J. O., Bårdsen, B. J., Wilson, J. G., Nikolaev, K. E., Sukhotin, A. A., Skírnisson, K., Saville, D. H., Ivanov, M. v., & Regel, K. v. (2015). Factors influencing the distribution of trematode larvae in blue mussels *Mytilus edulis* in the North Atlantic and Arctic Oceans. *Marine Biology*, 162(1), 193–206. <https://doi.org/10.1007/s00227-014-2586-4>
- Galaktionov, K. V., Nikolaev, K. E., Aristov, D. A., Levakin, I. A., & Kozminsky, E. V. (2019). Parasites on the edge: patterns of trematode transmission in the Arctic intertidal at the Pechora Sea (South-Eastern Barents Sea). *Polar Biology*, 42, 1719-1737. <https://doi.org/10.1007/s00300-018-2413-3>
- Galaktionov, K. V., Solovyeva, A. I., Blakeslee, A. M., & Skírnisson, K. (2023). Overview of *renicolid digeneans* (Digenea, Rencolidae) from marine gulls of northern Holarctic with remarks on their species statuses, phylogeny and phylogeography. *Parasitology*, 150(1), 55-77. doi: <https://doi.org/10.1017/S0031182022001500>
- Gosling, E. (2008). Bivalve molluscs: biology, ecology and culture. John Wiley & Sons.
- Granovitch, A. I., & Mikhailova, N. A. (2004). Rocky shore trematodes of the west coast of Sweden: distribution and life cycle strategies. *Acta Parasitol*, 49(3), 228-236. ISSN 1230-2821
- Haarpaintner, J., & Davids, C. (2021). Mapping Atmospheric Exposure of the Intertidal Zone with Sentinel-1 CSAR in Northern Norway. *Remote Sensing*, 13(17), 3354. <https://doi.org/10.3390/rs13173354>
- Hartig, F. (2022). DHARMA: Residual diagnostics for hierarchical (multi-level / mixed) models [R package version 0.4.6]. <https://CRAN.R-project.org/package=DHARMA>
- Hechinger, R. F., & Lafferty, K. D. (2005). Host diversity begets parasite diversity: bird final hosts and trematodes in snail intermediate hosts. *Proceedings of the Royal Society B: Biological Sciences*, 272(1567), 1059-1066. <https://doi.org/10.1098/rspb.2005.3070>
- Hilgerloh, G. (1997). Predation by birds on blue mussel *Mytilus edulis* beds of the tidal flats of Spiekeroog (southern North Sea). *Marine Ecology Progress Series*, 146, 61-72. <https://doi.org/10.3354/meps146061>
- Holmgren, M., & Scheffer, M. (2010). Strong facilitation in mild environments: the stress gradient hypothesis revisited. *Journal of Ecology*, 98(6), 1269-1275. <https://doi.org/10.1111/j.1365-2745.2010.01709.x>
- Horn, S., de La Vega, C., Asmus, R., Schwemmer, P., Enners, L., Garthe, S., Binder, K., & Asmus, H. (2017). Interaction between birds and macrofauna within food webs of six intertidal habitats of the Wadden Sea. *PLoS ONE*, 12(5). <https://doi.org/10.1371/journal.pone.0176381>

- Kamermans, P., & Saurel, C. (2022). Interacting climate change effects on mussels (*Mytilus edulis* and *M. galloprovincialis*) and oysters (*Crassostrea gigas* and *Ostrea edulis*): experiments for bivalve individual growth models. *Aquatic Living Resources*, 35(1), 296-304. <https://doi.org/10.1051/alr/2022001>
- Khosravi, M., Thieltges, D. W., Díaz-Morales, D. M., Bommarito, C., & Vajedsamiei, J. (2023). Filtration and respiration responses of mussels (*Mytilus edulis*) to trematode parasite infections (*Renicola roscovita*) and transient heat exposure. *International Journal for Parasitology: Parasites and Wildlife*, 21, 296–304. <https://doi.org/10.1016/j.ijppaw.2023.07.007>
- Krapivin, V. A., Bagrov, S. v., & Varfolomeeva, M. A. (2018). Effect of tidal level on abundance of symbionts in the White Sea blue mussel. *Diseases of Aquatic Organisms*, 130(2), 131–144. <https://doi.org/10.3354/dao03259>
- Lafferty, K. D. (1997). Environmental parasitology: what can parasites tell us about human impacts on the environment? *Parasitology today*, 13(7), 251-255. [https://doi.org/10.1016/S0169-4758\(97\)01072-7](https://doi.org/10.1016/S0169-4758(97)01072-7)
- Lafferty, K. D., Allesina, S., Arim, M., Briggs, C. J., De Leo, G., Dobson, A. P., ... & Thieltges, D. W. (2008). Parasites in food webs: the ultimate missing links. *Ecology letters*, 11(6), 533-546. <https://doi.org/10.1111/j.1461-0248.2008.01174.x>
- Landsberg, J. H., Blakesley, B. A., Reese, R. O., McRae, G., & Forstchen, P. R. (1998). Parasites of fish as indicators of environmental stress. *Environmental Monitoring and Assessment*, 51, 211-232. https://doi.org/10.1007/978-3-642-21396-0_12
- Lauckner, G. (1971). On the trematode fauna of the cockles *Cardium edule* and *Cardium lamarcki*. *Helgoländer wissenschaftliche Meeresuntersuchungen*, 22, 377-400. <https://doi.org/10.1007/BF01611126>
- Lauckner, G. (1983) Diseases of Mollusca: Bivalvia. In: Kinne, O. (ed) Diseases of marine animals, Vol 2: Introduction, Bivalvia to Scaphopoda. Biologische Anstalt Helgoland, Hamburg. [https://www.int-res.com/archive/doma_books/DOMA_Vol_II_\(bivalvia_to_arthropoda\).pdf](https://www.int-res.com/archive/doma_books/DOMA_Vol_II_(bivalvia_to_arthropoda).pdf)
- Lauckner, G. (1984). Impact of trematode parasitism on the fauna of a North Sea tidal flat. *Helgoländer Meeresuntersuchungen*, 37, 185-199. <https://doi.org/10.1007/BF01989303>
- Lawton, J. H., & Shachak, M. (1994). Organisms as ecosystem engineers. *Oikos*, 373-386. <https://doi.org/10.2307/3545850>
- Lefebvre, F., & Poulin, R. (2005). Progenesis in digenean trematodes: a taxonomic and synthetic overview of species reproducing in their second intermediate hosts. *Parasitology*, 130(6), 587-605. <https://doi.org/10.1017/S0031182004007103>
- Liddell, C., Welsh, J. E., van der Meer, J., & Thieltges, D. W. (2017). Effect of dose and frequency of exposure to infectious stages on trematode infection intensity and success in mussels. *Diseases of Aquatic Organisms*, 125(2), 85-92. <https://doi.org/10.3354/dao03133>

- Liénart, C., Garbaras, A., Qvarfordt, S., Sysoev, A. Ö., Högländer, H., Walve, J., ... & Karlson, A. M. (2021). Long-term changes in trophic ecology of blue mussels in a rapidly changing ecosystem. *Limnology and Oceanography*, 66(3), 694-710. <https://doi.org/10.1002/lno.11633>
- Lise, I., Bråte, N., Buenaventura, N., & Lusher, A. (2018). Occurrence of pearls in mussels (*Mytilus* spp.) from the Norwegian coast, 47. www.niva.no
- Loos-Frank, B. (1967). Experimentelle Untersuchungen über Bau, Entwicklung und Systematik der Himasthlinae (Trematoda, Echinostomatidae) des Nordseeraumes. *Zeitschrift für Parasitenkunde*, 28, 299-351. <https://doi.org/10.1007/BF00260294>
- Loos-Frank, B. (1969). Studies on the gymnophallid trematodes of the North Sea: I. The alternative life-cycles of *gymnophallus choledochus* Odhner, 1900. *Zeitschrift für Parasitenkunde*, 32, 135-156. <https://doi.org/10.1007/BF00259976>
- Loot, G., Aldana, M., & Navarrete, S. A. (2005). Effects of human exclusion on parasitism in intertidal food webs of central Chile. *Conservation Biology*, 19(1), 203-212. <https://dx.doi.org/10.1111/j.1523-1739.2005.00396.x>
- Maar, M., Larsen, J., Butenschön, M., Kristiansen, T., Thodsen, H., Taylor, D., & Schourup-Kristensen, V. (2024). Impacts of climate change on water quality, benthic mussels, and suspended mussel culture in a shallow, eutrophic estuary. *Heliyon*, 10(3). <https://doi.org/10.1016/j.heliyon.2024.e25218>
- Maire, O., Amouroux, J. M., Duchêne, J. C., & Grémare, A. (2007). Relationship between filtration activity and food availability in the Mediterranean mussel *Mytilus galloprovincialis*. *Marine Biology*, 152, 1293-1307. <https://doi.org/10.1007/s00227-007-0778-x>
- Marchiori, E., Quaglio, F., Franzo, G., Brocca, G., Aleksy, S., Cerchier, P., Cassini, R., & Marcer, F. (2023). Pearl formation associated with gymnophallid metacercariae in *Mytilus galloprovincialis* from the Northwestern Adriatic coast: Preliminary observations. *Journal of Invertebrate Pathology*, 196. <https://doi.org/10.1016/j.jip.2022.107854>
- Marcogliese, D. J. (2004). Parasites: Small Players with Crucial Roles in the Ecological Theater. *EcoHealth*, 1(2), 151–164. <https://doi.org/10.1007/s10393-004-0028-3>
- Marcogliese, D. J. (2005). Parasites of the superorganism: are they indicators of ecosystem health?. *International journal for parasitology*, 35(7), 705-716. <https://doi.org/10.1016/j.ijpara.2005.01.015>
- Marcogliese, D. J., & Cone, D. K. (1997). Food webs: a plea for parasites. *Trends in ecology & evolution*, 12(8), 320-325. [https://doi.org/10.1016/S0169-5347\(97\)01080-X](https://doi.org/10.1016/S0169-5347(97)01080-X)
- Moore, C. S., Gittman, R. K., Puckett, B. J., Wellman, E. H., & Blakeslee, A. M. H. (2020). If you build it, they will come: Restoration positively influences free-living and parasite diversity in a restored tidal marsh. *Food Webs*, 25, e00167. <https://doi.org/10.1016/j.fooweb.2020.e00167>

- Morley, N. J. (2012). Cercariae (Platyhelminthes: Trematoda) as neglected components of zooplankton communities in freshwater habitats. *Hydrobiologia*, Vol. 691(1), 7–19. <https://doi.org/10.1007/s10750-012-1029-9>
- Mouritsen, K. N., Dalsgaard, N. P., Flensburg, S. B., Madsen, J. C., & Selbach, C. (2022). Fear of parasitism affects the functional role of ecosystem engineers. *Oikos*, 2022(5), e08965. <https://doi.org/10.1111/oik.08965>
- Nagarajan, R., Lea, S. E. G., & Goss-Custard, J. D. (2006). Seasonal variations in mussel, *Mytilus edulis* L. shell thickness and strength and their ecological implications. *Journal of Experimental Marine Biology and Ecology*, 339(2), 241–250. <https://doi.org/10.1016/j.jembe.2006.08.001>
- Nikolaev, K. E., Prokofiev, V. v., Levakin, I. A., & Galaktionov, K. v. (2017). How the position of mussels at the intertidal lagoon affects their infection with the larvae of parasitic flatworms (Trematoda: Digenea): A combined laboratory and field experimental study. *Journal of Sea Research*, 128, 32–40. <https://doi.org/10.1016/j.seares.2017.07.010>
- Place, S. P., O'Donnell, M. J., & Hofmann, G. E. (2008). Gene expression in the intertidal mussel *Mytilus californianus*: physiological response to environmental factors on a biogeographic scale. *Marine Ecology Progress Series*, 356, 1-14. <https://doi.org/10.3354/meps07354>
- Poulin, R., & Leung, T. L. F. (2011). Latitudinal gradient in the taxonomic composition of parasite communities. *Journal of Helminthology*, 85(3), 228-233. <https://doi.org/10.1017/S0022149X10000696>
- Prinz, K., Kelly, T. C., O'Riordan, R. M., & Culloty, S. C. (2009). Non-host organisms affect transmission processes in two common trematode parasites of rocky shores. *Marine Biology*, 156, 2303-2311. <https://doi.org/10.1007/s00227-009-1258-2>
- Prinz, K., Kelly, T. C., O'Riordan, R. M., & Culloty, S. C. (2011). Factors influencing cercarial emergence and settlement in the digenean trematode *Parorchis acanthus* (Philophthalmidae). *Journal of the Marine Biological Association of the United Kingdom*, 91(8), 1673-1679. <https://doi.org/10.1017/S0025315410000718>
- Prokofiev, V. V., Galaktionov, K. V., & Levakin, I. A. (2016). Patterns of parasite transmission in polar seas: daily rhythms of cercarial emergence from intertidal snails. *Journal of Sea Research*, 113, 85-98. <https://doi.org/10.1016/j.seares.2015.07.007>
- Puljas, S., & Burazin, J. (2022). Infection of *Mytilus Galloprovincialis* by the Trematode *Parvatrema* sp. (Digenea: Gymnophallidae) in the Middle Adriatic Sea, Croatia. *Thalassas: An International Journal of Marine Sciences*, 38(2), 745-752. <https://doi.org/10.1007/s41208-022-00415-7>
- Raffel, T. R., Hoverman, J. T., Halstead, N. T., Michel, P. J., & Rohr, J. R. (2010). Parasitism in a community context: trait-mediated interactions with competition and predation. *Ecology*, 91(7), 1900-1907. <https://doi.org/10.1890/09-1697.1>
- Ryang, Y. S., Yoo, J. C., Lee, S. H., & Chai, J. Y. (2000). The palearctic oystercatcher *Haematopus ostralegus*, a natural definitive host for *Gymnophalloides seoi*. *Journal of*

Parasitology, 86(2), 418-419. [https://doi.org/10.1645/0022-3395\(2000\)086\[0418:TPOHOA\]2.0.CO;2](https://doi.org/10.1645/0022-3395(2000)086[0418:TPOHOA]2.0.CO;2)

- Selbach, C., Barsøe, M., Vogensen, T. K., Samsing, A. B., & Mouritsen, K. N. (2020). Temperature–parasite interaction: do trematode infections protect against heat stress? *International Journal for Parasitology*, 50(14), 1189–1194. <https://doi.org/10.1016/j.ijpara.2020.07.006>
- Selbach, C., de Framond-Benard, E., & Mouritsen, K. N. (2024). Under the cover of ice: Trematode infections affect survival and growth of wintering mussels. *Marine Ecology Progress Series*, 740, 213-218. <https://doi.org/10.3354/meps14638>
- Sellæg, V. (2023). Drivers of an unexpected unimodal vertical pattern in size distribution of intertidal blue mussels (*Mytilus* spp.). [Master's Thesis, Arctic University of Tromsø]. <https://hdl.handle.net/10037/32148>
- Shick, J. M., Gnaiger, E., Widdows, J., Bayne, B. L., & De Zwaan, A. (1986). Activity and metabolism in the mussel *Mytilus edulis* L. during intertidal hypoxia and aerobic recovery. *Physiological zoology*, 59(6), 627-642.
- Shields, J. L., Barnes, P., & Heath, D. D. (2008). Growth and survival differences among native, introduced and hybrid blue mussels (*Mytilus* spp.): genotype, environment and interaction effects. *Marine Biology*, 154(5), 919-928. <https://doi.org/10.1086/physzool.59.6.30158610>
- Stachowicz, J. J. (2001). Mutualism, facilitation, and the structure of ecological communities: positive interactions play a critical, but underappreciated, role in ecological communities by reducing physical or biotic stresses in existing habitats and by creating new habitats on which many species depend. *Bioscience*, 51(3), 235-246. [https://doi.org/10.1641/0006-3568\(2001\)051\[0235:MFATSO\]2.0.CO;2](https://doi.org/10.1641/0006-3568(2001)051[0235:MFATSO]2.0.CO;2)
- Stier, T., Drent, J., Thielgtes, D.W. (2015) Trematode infections reduce clearance rates and condition in blue mussels *Mytilus edulis*. *Marine Ecology Progress Series*, 529, 137-144. <https://doi.org/10.3354/meps11250>
- Studer, A., & Poulin, R. (2012). Seasonal dynamics in an intertidal mudflat: the case of a complex trematode life cycle. *Marine Ecology Progress Series*, 455, 79–93. <https://doi.org/10.3354/meps09761>
- Studer, A., Widmann, M., Poulin, R., & Krkošek, M. (2013). Large scale patterns of trematode parasitism in a bivalve host: no evidence for a latitudinal gradient in infection levels. *Marine Ecology Progress Series*, 491, 125-135. <https://doi.org/10.3354/meps10483>
- Stunkard, H. W. (1932). Some larval Trematodes from the coast in the region of Roscoff, Finisterre. *Parasitology*. 24, 321–343. <https://doi.org/10.1017/S0031182000020746>
- Stunkard, H. W. (1971). Renicolid trematodes (Digenea) from the renal tubules of birds. *Annales de Parasitologie Humaine et Comparée*, 46(1), 109-118. <https://doi.org/10.1051/parasite/1971461109>

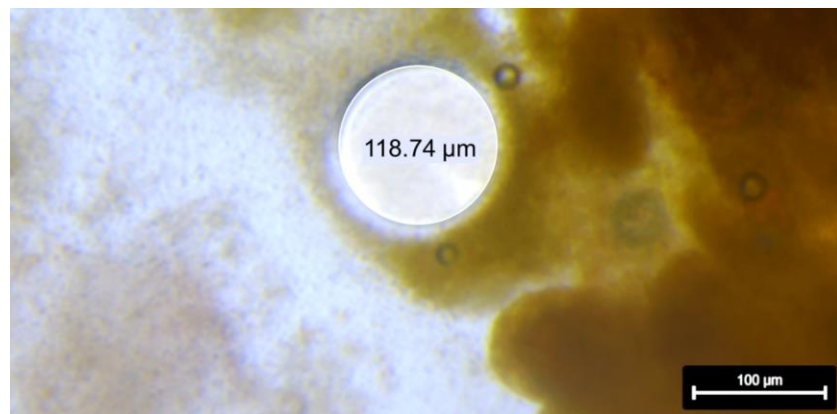
- Sukhdeo, M. V. (2010). Food webs for parasitologists: a review. *Journal of Parasitology*, 96(2), 273-284. <https://doi.org/10.1645/GE-2254.1>
- Svårdh, L. (1999). Bacteria, granulocytomas, and trematode metacercariae in the digestive gland of *Mytilus edulis*: seasonal and interpopulation variation. *Journal of Invertebrate Pathology*, 74(3), 275-280. <https://doi.org/10.1006/jipa.1999.4880>
- Szidat, L. (1962). Über eine ungewöhnliche Parthenogenetischer Vermehrung bei metacecarien einer Gymnophallus-Art aus *Mytilus PLatensis*, *Gymnophallus Australis* N. sp. Des Südatlantik [On an unusual parthenogenetic reproduction in metacercariae of a Gymnophallus species from *Mytilus platensis*, *Gymnophallus australis* n. sp. of the South Atlantic]. *Parasitology*, 22, 196–213. <https://doi.org/10.1007/s11230-007-9105-7>
- Thieltges, D. W. (2006). Effect of infection by the metacercarial trematode *Renicola roscovita* on growth in intertidal blue mussel *Mytilus edulis*. *Marine Ecology Progress Series*, 319, 129-134. <https://doi.org/10.3354/MEPS319129>
- Thieltges, D. W. (2007). Habitat and transmission–effect of tidal level and upstream host density on metacercarial load in an intertidal bivalve. *Parasitology*, 134(4), 599-605. <https://doi.org/10.1017/S003118200600165X>
- Thieltges, D. W., & Reise, K. (2007). Spatial heterogeneity in parasite infections at different spatial scales in an intertidal bivalve. *Oecologia*, 150, 569-581. <https://doi.org/10.1007/s00442-006-0557-2>
- Thieltges, D. W., & Rick, J. (2006). Effect of temperature on emergence, survival and infectivity of cercariae of the marine trematode *Renicola roscovita* (Digenea: Rencolidae). *Diseases of aquatic organisms*, 73(1), 63-68. <https://doi.org/10.3354/dao073063>
- Thieltges, D. W., Jensen, K. T., Poulin, R. (2008) The role of biotic factors in the transmission of free-living endohelminth stages. *Parasitology*, 135, 407–426. [doi:10.1017/S0031182007000248](https://doi.org/10.1017/S0031182007000248)
- Thieltges, D. W., Johnson, P. T., van Leeuwen, A., & Koprivnikar, J. (2024). Effects of predation risk on parasite–host interactions and wildlife diseases. *Ecology*, 105(6), e4315. <https://doi.org/10.1002/ecy.4315>
- Thornsnæs G., Svendsen T. O., Engerengen L., SNL (accessed: 24.11.2023) <https://snl.no/Troms%C3%B8>
- Tolman, D., Wood, H. L., Skibinski, D. O., & Truebano, M. (2019). Differential immunity as a factor influencing mussel hybrid zone structure. *Marine biology*, 166(12), 151.
- Walsh, J. E. (2008). Climate of the Arctic marine environment. *Ecological applications*, 18(2), 3-22. <https://doi.org/10.1890/06-0503.1>
- Welsh, J. E., van der Meer, J., Brussaard, C. P., & Thieltges, D. W. (2014). Inventory of organisms interfering with transmission of a marine trematode. *Journal of the Marine Biological Association of the United Kingdom*, 94(4), 697-702. <https://doi.org/10.1017/S0025315414000034>

- Werding, B. (1969). Morphologie, entwicklung und ökologie digener trematoden-larven der strandschnecke *Littorina littorea*. *Marine biology*, 3, 306-333. <https://doi.org/10.1007/BF00698861>
- Werner, E. E., & Peacor, S. D. (2003). A review of trait-mediated indirect interactions in ecological communities. *Ecology*, 84(5), 1083-1100. [https://doi.org/10.1890/0012-9658\(2003\)084](https://doi.org/10.1890/0012-9658(2003)084)
- Wickham, H. (2016). *ggplot2: Elegant Graphics for Data Analysis*. Springer-Verlag New York.
- Widdows, J., & Shick, J. M. (1985). Physiological responses of *Mytilus edulis* and *Cardium edule* to aerial exposure. *Marine Biology*, 85(3), 217-232. <https://doi.org/10.1007/BF00393242>
- Wilson, J. G., Galaktionov, K. v., Sukhotin, A. A., Skirnisson, K., Nikolaev, K. E., Ivanov, M. I., Bustnes, J. O., Saville, D. H., & Regel, K. v. (2013). Factors influencing trematode parasite burdens in mussels (*Mytilus* spp) from the north Atlantic ocean across to the north Pacific. *Estuarine, Coastal and Shelf Science*, 132, 87–93. <https://doi.org/10.1016/j.ecss.2011.10.005>
- WoRMS Editorial Board (2024). World Register of Marine Species. <https://www.marinespecies.org> at VLIZ. Accessed: 12.08.2024. doi:10.14284/170
- Jones, C. G., Wright, C. A. (1960). Relationships between trematodes and molluscs. *Annals of Tropical Medicine and Parasitology*, 54(1), 1–7. <https://doi.org/10.1080/00034983.1960.11685951>
- Yee, T. W. (2024). VGAM: Vector Generalized Linear and Additive Models. R package version 1.1-11, <https://CRAN.R-project.org/package=VGAM>.

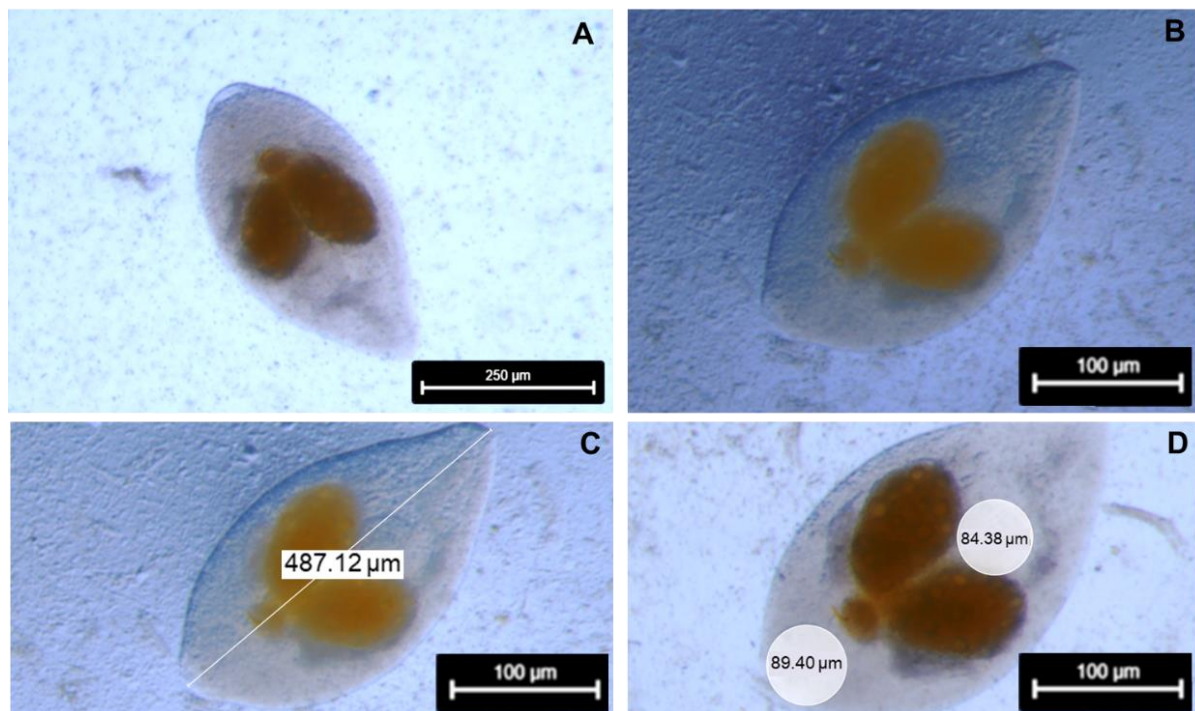
6. Appendix

Appendix 1 – When measuring salinity at sampling sites, a manual ATC refractometer (Kern&Sohn, Germany) as well as a digital refractometer, PA203 (Misco, US), were used, and the value obtained is reported in Practical Salinity Units (PSU).

| Season | SOM1 | SOM2 | SOM3 | SOM4 |
|--------|---------|---------|---------|---------|
| winter | 35/35 | 35/35 | 34/34 | 36/36 |
| spring | 35/35 | 29/28 | 36/37 | 35/36 |
| summer | 35/34 | 35/34 | 36/35 | 35/35 |
| fall | 33.5/28 | 34.5/28 | 35.5/35 | 36.5/36 |



Appendix 2 – Metacercaria of *Renicola* sp. found in the digestive gland of *Mytilus* sp. at SOM2 during fall., The diameter is approximately 119 μm for this individual.



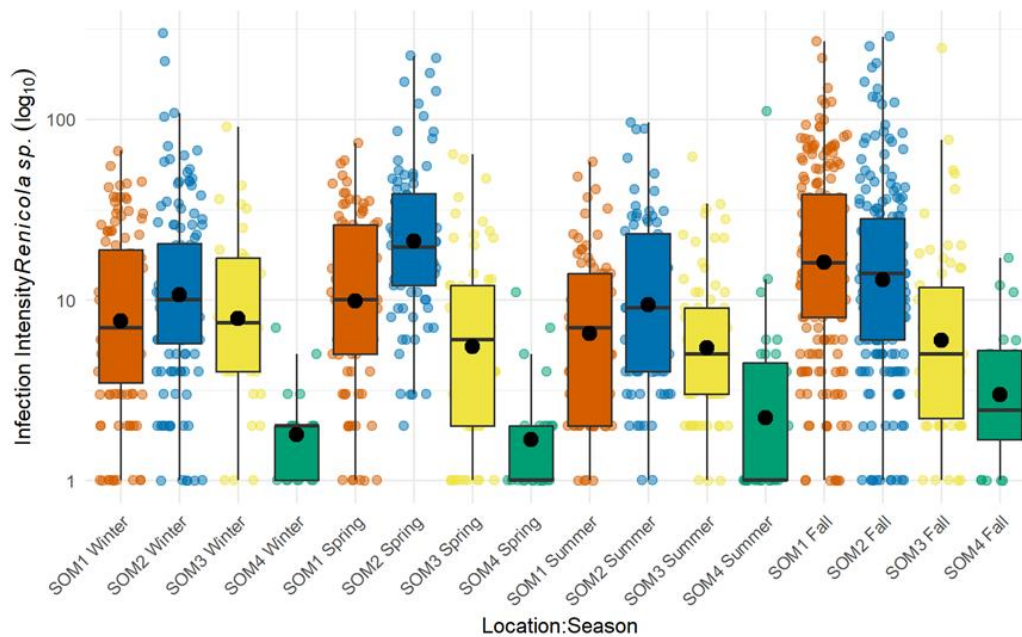
Appendix. 3 – **A)** Dorsal view of metacercariae of *Gymnophallus* sp; **B)** Ventral view on *Gymnophallus* sp. metacercariae **C)** Body length of *Gymnophallus* sp. metacercariae ~490 μm **D)** Suckers of *Gymnophallus* sp. with a diameter of 85 μm (ventral) and 89 μm (oral) for this individual.

Appendix 4 - Zero truncated negative binomial generalized linear model showing differences between sampling locations and among seasons in infection intensity with *Renicola* sp. Values given are (from left to right): model estimate; standard error, z-value, and p-value.

| vglm(Renicola_sp. ~ Location + Season + Length, family = posnegbinomial(),data) | | | | |
|---|--------------|-------------|---------------|------------------|
| | Estimate | Std. Error | z value | Pr(> z) |
| (Intercept):1 | 1.17 | 0.25 | 4.68 | <0.001 |
| (Intercept):2 | -0.49 | 0.07 | -6.94 | <0.001 |
| LocationSOM2 | 0.26 | 0.08 | 3.06 | 0.002 |
| LocationSOM3 | -0.71 | 0.11 | -6.30 | <0.001 |
| LocationSOM4 | -1.90 | 0.16 | -11.66 | <0.001 |
| SeasonSpring | -0.20 | 0.10 | -1.92 | 0.054 |
| SeasonSummer | -0.21 | 0.12 | -1.79 | 0.074 |
| SeasonWinter | -0.45 | 0.10 | -4.56 | <0.001 |
| Length | 0.06 | 0.01 | 7.91 | <0.001 |

Appendix 5 - Zero truncated negative binomial generalized linear model showing interactive effects of sampling location and season sampled in infection intensity of *Renicola* sp. Values given are (from left to right): model estimate; standard error, z-value, and p-value.

| vglm(Renicola_sp. ~ Location + Season + Length+Location*Season, family = posnegbinomial(),data) | | | | |
|---|--------------|-------------|--------------|------------------|
| | Estimate | Std. Error | z value | Pr(> z) |
| (Intercept):1 | 1.18 | 0.25 | 4.71 | <0.001 |
| (Intercept):2 | -0.40 | 0.07 | -5.91 | <0.001 |
| LocationSOM2 | -0.15 | 0.13 | -1.19 | 0.235 |
| LocationSOM4 | -2.82 | 0.31 | -9.03 | <0.001 |
| LocationSOM3 | -1.14 | 0.19 | -6.02 | <0.001 |
| SeasonWinter | -0.77 | 0.15 | -5.19 | <0.001 |
| SeasonSummer | -0.73 | 0.18 | -4.15 | <0.001 |
| SeasonSpring | -0.64 | 0.16 | -3.90 | <0.001 |
| Length | 0.07 | 0.01 | 8.91 | <0.001 |
| LocationSOM2:SeasonWinter | 0.50 | 0.20 | 2.49 | 0.013 |
| LocationSOM4:SeasonWinter | -0.23 | 0.49 | -0.48 | 0.632 |
| LocationSOM3:SeasonWinter | 1.05 | 0.30 | 3.46 | 0.001 |
| LocationSOM2:SeasonSummer | 0.57 | 0.24 | 2.40 | 0.017 |
| LocationSOM4:SeasonSummer | 2.03 | 0.41 | 5.01 | <0.001 |
| LocationSOM3:SeasonSummer | 0.81 | 0.28 | 2.90 | 0.004 |
| LocationSOM2:SeasonSpring | 1.02 | 0.23 | 4.46 | <0.001 |
| LocationSOM4:SeasonSpring | 0.40 | 0.46 | 0.88 | 0.377 |
| LocationSOM3:SeasonSpring | 0.35 | 0.27 | 1.28 | 0.201 |



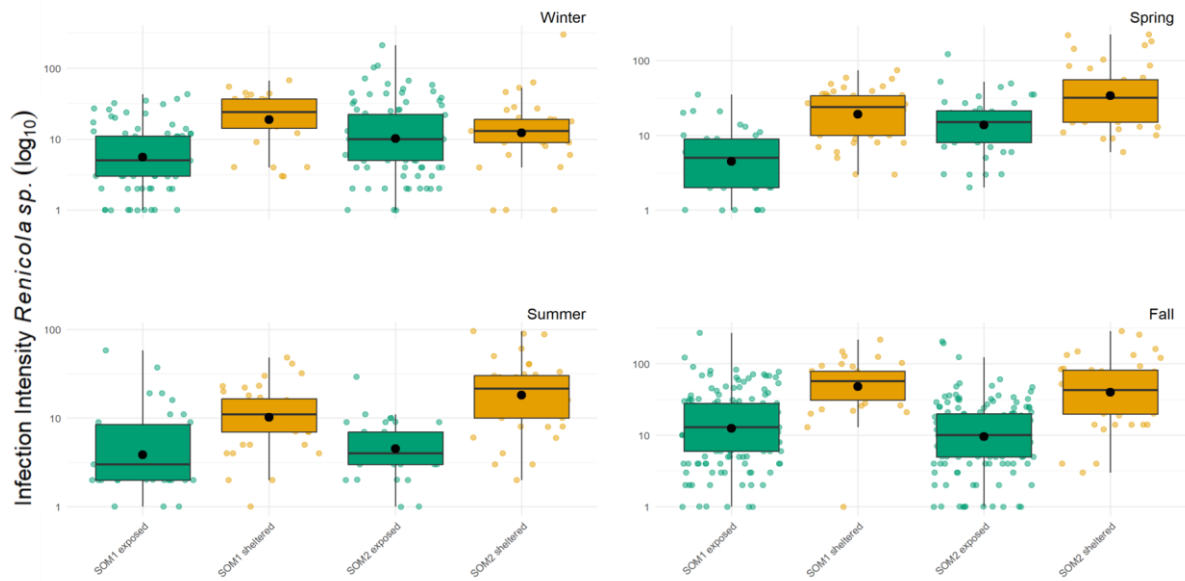
Appendix 6 - Infection intensity of *Renicola* sp. displayed in boxplots on a log₁₀ scale, displayed by location and season (SOM1 orange, SOM2 blue, SOM3 yellow, SOM4 green). The vertical line within each boxplot represents the median at that location, and the dark point indicates the mean. Each point in the scatterplot represents the infection intensity for an individual sampled blue mussel.

Appendix 7 - Zero truncated negative binomial generalized linear model showing effects of wave exposure on infection intensity of *Renicola* sp.. Values given are (from left to right): model estimate; standard error, z-value, and p-value.

| vglm(Renicola_sp.~ Wave_exposure+Length,family = posnegbinomial(),data) | | | | | |
|---|-------------|-------------|--------------|------------------|--|
| | Estimate | Std. Error | z value | Pr(> z) | |
| (Intercept):1 | -0.34 | 0.21 | -1.58 | 0.115 | |
| (Intercept):2 | -0.08 | 0.07 | -1.24 | 0.215 | |
| Wave_exposuresheltered | 0.87 | 0.07 | 11.69 | <0.001 | |
| Length | 0.11 | 0.01 | 14.12 | <0.001 | |

Appendix 8 - Zero truncated negative binomial generalized linear model showing interactive effects of wave exposure and sampling location as well as wave exposure and season on infection intensity of *Renicola* sp. Values given are (from left to right): model estimate; standard error, z-value, and p-value.

| vglm(Renicola_sp.~ Wave_exposure+Length+Wave_exposure*Location+Wave_exposure*Season,family = posnegbinomial(),data) | | | | | |
|---|--------------|-------------|--------------|------------------|--|
| | Estimate | Std. Error | z value | Pr(> z) | |
| (Intercept):1 | 0.34 | 0.25 | 1.38 | 0.167 | |
| (Intercept):2 | 0.02 | 0.06 | 0.36 | 0.717 | |
| Wave_exposuresheltered | 0.95 | 0.15 | 6.31 | <0.001 | |
| Length | 0.09 | 0.01 | 10.54 | <0.001 | |
| LocationSOM2 | -0.03 | 0.08 | -0.37 | 0.710 | |
| SeasonSpring | -0.18 | 0.13 | -1.36 | 0.174 | |
| SeasonSummer | -0.70 | 0.15 | -4.60 | <0.001 | |
| SeasonWinter | -0.22 | 0.10 | -2.19 | 0.028 | |
| Wave_exposuresheltered:LocationSOM2 | 0.47 | 0.15 | 3.19 | 0.001 | |
| Wave_exposuresheltered:SeasonSpring | -0.37 | 0.21 | -1.81 | 0.071 | |
| Wave_exposuresheltered:SeasonSummer | -0.09 | 0.22 | -0.40 | 0.687 | |
| Wave_exposuresheltered:SeasonWinter | -0.67 | 0.20 | -3.38 | 0.001 | |



Appendix 9 - Infection intensity of *Renicola* sp. displayed in boxplots on a \log_{10} scale, displayed by location and wave exposure (wave exposed green, wave-sheltered orange) throughout different seasons. The vertical line within each boxplot represents the median at that location, and the dark point indicates the mean. Each point in the scatterplot represents the infection intensity for an individual sampled blue mussel.

Appendix 10 - Zero truncated negative binomial generalized linear model showing the differences among the various intertidal levels, top; high; mid, and low on infection intensity of *Renicola* sp. Values given are (from left to right): model estimate; standard error, z-value, and p-value.

| vglm(Renicola_sp.~ intertidal level+Length,family = posnegbinomial(),data) | | | | |
|--|----------|------------|---------|----------|
| | Estimate | Std. Error | z value | Pr(> z) |
| (Intercept):1 | 0.95 | 0.35 | 2.73 | 0.006 |
| (Intercept):2 | -0.14 | 0.10 | -1.46 | 0.145 |
| Intertidal_levellow | 0.69 | 0.15 | 4.70 | <0.001 |
| Intertidal_levelmid | 0.39 | 0.14 | 2.80 | 0.005 |
| Intertidal_leveltop | -0.22 | 0.15 | -1.50 | 0.134 |
| Length | 0.05 | 0.01 | 4.55 | <0.001 |

Appendix 11 - Zero truncated negative binomial generalized linear model showing interactive effects of intertidal level and season as well as intertidal level and location on infection intensity with *Renicola* sp. Values given are (from left to right): model estimate; standard error, z-value, and p-value.

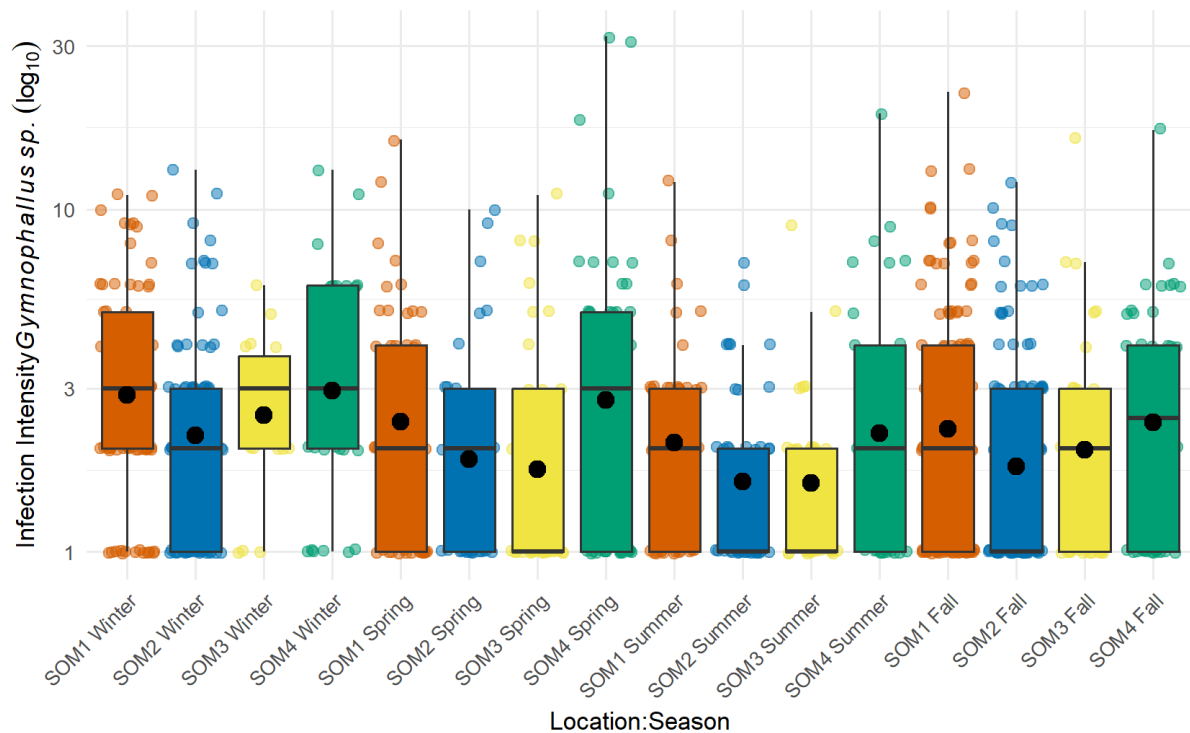
| vglm(Renicola_sp.~ Intertidal_level+Length Intertidal_level*Location+Intertidal_level*Season,family = posnegbinomial(),data) | | | | |
|--|--------------|-------------|--------------|------------------|
| | Estimate | Std. Error | z value | Pr(> z) |
| (Intercept):1 | 0.79 | 0.36 | 2.17 | 0.030 |
| (Intercept):2 | 0.08 | 0.09 | 0.86 | 0.390 |
| Intertidal_levellow | 0.33 | 0.22 | 1.52 | 0.129 |
| Intertidal_levelmid | -0.42 | 0.21 | -2.02 | 0.043 |
| Intertidal_leveltop | -0.02 | 0.21 | -0.10 | 0.917 |
| Length | 0.07 | 0.01 | 6.18 | <0.001 |
| LocationSOM2 | -0.24 | 0.19 | -1.22 | 0.221 |
| SeasonWinter | -1.17 | 0.20 | -5.93 | <0.001 |
| Intertidal_levellow:LocationSOM2 | -0.06 | 0.27 | -0.21 | 0.832 |
| Intertidal_levelmid:LocationSOM2 | 0.85 | 0.26 | 3.29 | 0.001 |
| Intertidal_leveltop:LocationSOM2 | -0.94 | 0.27 | -3.46 | 0.001 |
| Intertidal_levellow:SeasonWinter | 1.21 | 0.27 | 4.42 | <0.001 |
| Intertidal_levelmid:SeasonWinter | 1.16 | 0.26 | 4.40 | <0.001 |
| Intertidal_leveltop:SeasonWinter | 0.85 | 0.29 | 2.94 | 0.003 |

Appendix 12 - Zero truncated positive negative binomial generalized linear model showing differences in infection intensity of *Gymnophallus* sp. between sampling locations and seasons. Values given are (from left to right): model estimate; standard error, z-value, and p-value.

| vglm(Gymnophallus_sp.~ Location+Season+Length,family = posnegbinomial(),data) | | | | |
|---|--------------|-------------|--------------|------------------|
| | Estimate | Std. Error | z value | Pr(> z) |
| (Intercept):1 | 0.08 | 0.38 | 0.21 | 0.836 |
| (Intercept):2 | -0.72 | 0.24 | -2.97 | 0.003 |
| SiteSOM2 | -0.47 | 0.13 | -3.54 | <0.001 |
| SiteSOM3 | -0.49 | 0.18 | -2.80 | 0.005 |
| SiteSOM4 | 0.22 | 0.16 | 1.34 | 0.181 |
| SeasonSpring | 0.18 | 0.15 | 1.18 | 0.238 |
| SeasonSummer | -0.21 | 0.18 | -1.20 | 0.230 |
| SeasonWinter | 0.29 | 0.14 | 2.04 | 0.041 |
| Length | 0.01 | 0.01 | 1.10 | 0.273 |

Appendix 13 - Zero truncated negative binomial generalized linear model showing interactive effects of season and location on infection intensity with *Gymnophallus* sp. Values given are (from left to right): model estimate; standard error, z-value, and p-value.

| vglm(Gymnophallus_sp.~ Location+Season+Length+Location*Season,family = posnegbinomial(),data) | | | | |
|---|--------------|-------------|--------------|--------------|
| | Estimate | Std. Error | z value | Pr(> z) |
| (Intercept):1 | -0.03 | 0.39 | -0.07 | 0.941 |
| (Intercept):2 | -0.67 | 0.24 | -2.85 | 0.004 |
| LocationSOM3 | -0.38 | 0.30 | -1.24 | 0.215 |
| LocationSOM2 | -0.52 | 0.20 | -2.57 | 0.010 |
| LocationSOM4 | -0.16 | 0.27 | -0.59 | 0.553 |
| SeasonSpring | 0.03 | 0.25 | 0.11 | 0.914 |
| SeasonWinter | 0.24 | 0.22 | 1.10 | 0.272 |
| SeasonSummer | -0.18 | 0.28 | -0.65 | 0.516 |
| Length | 0.02 | 0.01 | 1.58 | 0.114 |
| LocationSOM3:SeasonSpring | -0.20 | 0.44 | -0.45 | 0.654 |
| LocationSOM2:SeasonSpring | 0.09 | 0.39 | 0.23 | 0.816 |
| LocationSOM4:SeasonSpring | 0.71 | 0.39 | 1.81 | 0.071 |
| LocationSOM3:SeasonWinter | -0.05 | 0.49 | -0.10 | 0.918 |
| LocationSOM2:SeasonWinter | 0.12 | 0.32 | 0.39 | 0.697 |
| LocationSOM4:SeasonWinter | 0.20 | 0.41 | 0.49 | 0.627 |
| LocationSOM3:SeasonSummer | -0.26 | 0.49 | -0.54 | 0.587 |
| LocationSOM2:SeasonSummer | -0.08 | 0.40 | -0.19 | 0.846 |
| LocationSOM4:SeasonSummer | 0.41 | 0.44 | 0.93 | 0.350 |



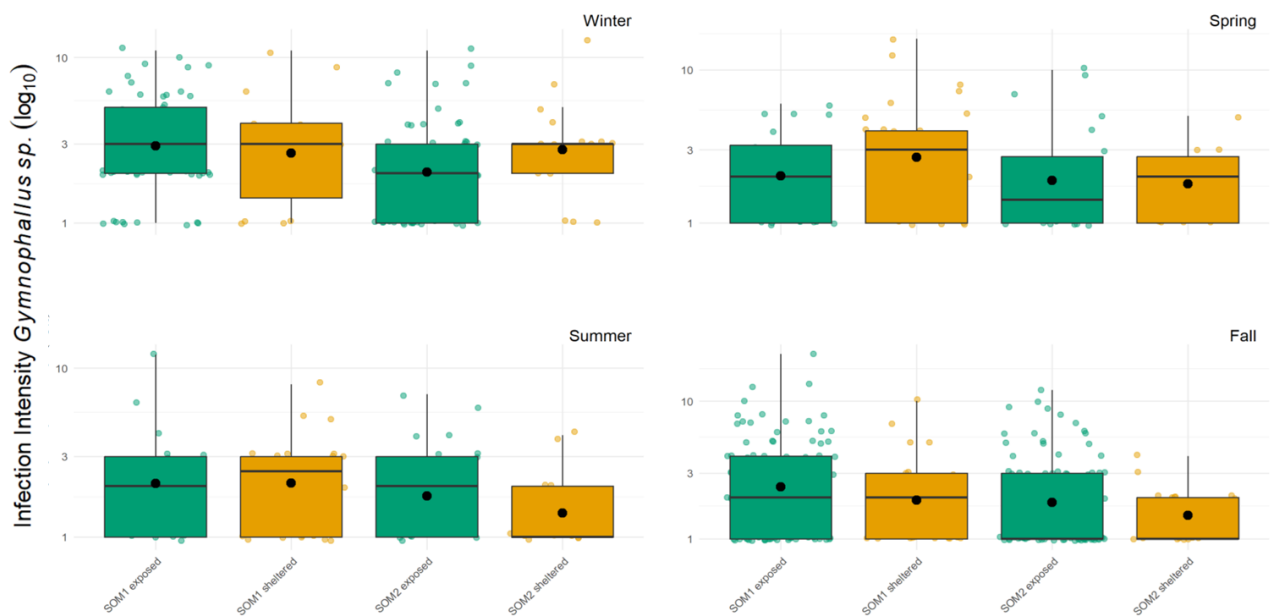
Appendix 14 - Infection intensity of *Gymnophallus* sp. at different locations throughout all seasons on a log₁₀ scale (SOM1 orange, SOM2 blue, SOM3 yellow, SOM4 green). Displayed in a histogram with singular samples plotted with a colored dot. The black line represents the median while the black dots represent the mean infection intensity at each location.

Appendix 15 - Zero truncated negative binomial generalized linear model showing effects of wave exposure on infection intensity of *Gymnophallus* sp. Values given are (from left to right): model estimate; standard error, z-value, and p-value.

| vglm(<i>Gymnophallus</i> _sp.~ Wave_exposure+Length,family = posnegbinomial(),data) | | | | |
|--|----------|------------|---------|----------|
| | Estimate | Std. Error | z value | Pr(> z) |
| (Intercept):1 | -0.03 | 0.43 | -0.07 | 0.944 |
| (Intercept):2 | -0.68 | 0.30 | -2.25 | 0.024 |
| Wave_exposuresheltered | -0.10 | 0.14 | -0.73 | 0.465 |
| Length | 0.01 | 0.01 | 1.01 | 0.311 |

Appendix 16 - Zero truncated positive negative binomial generalized linear model showing interactive effects of wave exposure and sampling location as well as wave exposure and season on infection intensity with *Renicola* sp. Values given are (from left to right): model estimate; standard error, z-value, and p-value.

| vglm(Gymnophallus_sp.~ Wave_exposure +Length+ Wave_exp.*Location+ Wave_exp.*Season, family = posnegbinomial(),data) | | | | |
|---|--------------|-------------|--------------|--------------|
| | Estimate | Std. Error | z value | Pr(> z) |
| (Intercept):1 | 0.36 | 0.47 | 0.77 | 0.442 |
| (Intercept):2 | -0.39 | 0.26 | -1.48 | 0.140 |
| Wave_exposuresheltered | -0.52 | 0.28 | -1.81 | 0.070 |
| Length | 0.01 | 0.02 | 0.73 | 0.465 |
| LocationSOM2 | -0.43 | 0.15 | -2.87 | 0.004 |
| SeasonSpring | -0.11 | 0.25 | -0.45 | 0.649 |
| SeasonSummer | -0.20 | 0.27 | -0.76 | 0.446 |
| SeasonWinter | 0.14 | 0.17 | 0.85 | 0.393 |
| Wave_exposuresheltered:LocationSOM2 | -0.23 | 0.29 | -0.80 | 0.421 |
| Wave_exposuresheltered:SeasonSpring | 0.73 | 0.41 | 1.80 | 0.072 |
| Wave_exposuresheltered:SeasonSummer | 0.27 | 0.42 | 0.64 | 0.520 |
| Wave_exposuresheltered:SeasonWinter | 0.85 | 0.37 | 2.26 | 0.024 |



Appendix 17- Infection intensity of *Gymnophallus* sp. at different locations with varying wave-exposures (Wave-exposed green, Wave-sheltered orange) throughout all seasons on a log₁₀ scale. Displayed in a histogram with singular samples plotted with a colored dot. The black line represents the median while the black dots represent the mean infection intensity at each location.

Appendix 18 - Zero truncated negative binomial generalized linear model showing the differences among the various intertidal levels, top; high; mid, and low on infection intensity of *Gymnophallus* sp. Values given are (from left to right): model estimate; standard error, z-value, and p-value.

| vglm(Gymnophallus_sp.~ Intertidal_level+Length,family = posnegbinomial(),data) | | | | |
|--|--------------|-------------|--------------|--------------|
| | Estimate | Std. Error | z value | Pr(> z) |
| (Intercept):1 | 0.59 | 0.66 | 0.89 | 0.374 |
| (Intercept):2 | -0.64 | 0.38 | -1.69 | 0.090 |
| Intertidal_levelmid | -0.24 | 0.23 | -1.04 | 0.299 |
| Intertidal_leveltop | -0.05 | 0.24 | -0.20 | 0.845 |
| Intertidal_levellow | -0.15 | 0.26 | -0.59 | 0.558 |
| Length | 0.00 | 0.02 | -0.06 | 0.951 |

Appendix 19 - Zero truncated negative binomial generalized linear model showing interactive effects of intertidal level and season as well as intertidal level and location on infection intensity with *Gymnophallus* sp. Values given are (from left to right): model estimate; standard error, z-value, and p-value.

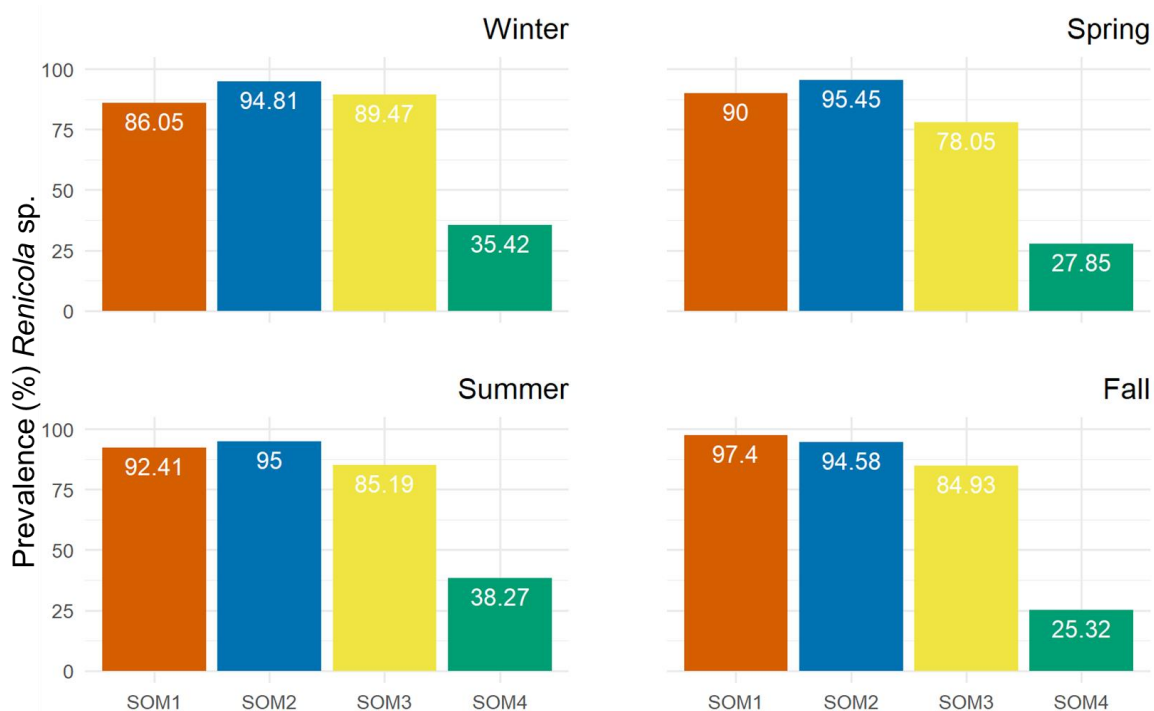
| vglm(Gymnophallus_sp.~ (Intertidal_level+Length+Intert._level*Location+Intert._level*Season),family = posnegbinomial(),data) | | | | |
|--|----------|------------|---------|----------|
| | Estimate | Std. Error | z value | Pr(> z) |
| (Intercept):1 | 0.38 | 0.70 | 0.55 | 0.583 |
| (Intercept):2 | -0.43 | 0.34 | -1.26 | 0.208 |
| Intertidal_levellow | -0.20 | 0.37 | -0.54 | 0.588 |
| Intertidal_levelmid | -0.07 | 0.35 | -0.19 | 0.850 |
| Intertidal_leveltop | -0.10 | 0.37 | -0.26 | 0.791 |
| Length | 0.01 | 0.02 | 0.61 | 0.542 |
| LocationSOM2 | -0.48 | 0.32 | -1.49 | 0.135 |
| SeasonWinter | 0.13 | 0.32 | 0.42 | 0.675 |
| Intertidal_levellow:LocationSOM2 | -0.12 | 0.49 | -0.24 | 0.813 |
| Intertidal_levelmid:LocationSOM2 | -0.06 | 0.45 | -0.13 | 0.899 |
| Intertidal_leveltop:LocationSOM2 | 0.05 | 0.45 | 0.11 | 0.914 |
| Intertidal_levellow:SeasonWinter | 0.26 | 0.51 | 0.51 | 0.613 |
| Intertidal_levelmid:SeasonWinter | -0.34 | 0.45 | -0.76 | 0.445 |
| Intertidal_leveltop:SeasonWinter | 0.22 | 0.46 | 0.48 | 0.634 |

Appendix 20 - Logistic regression model showing differences in prevalence between sampling locations and between seasons of *Renicola* sp. Values given are (from left to right): model estimate; standard error, z-value, and p-value.

| glm(Renicola_sp._Bin ~ Location+Season+Length+Location*Season, family = binomial (link = "logit") ,data) | | | | |
|--|--------------|-------------|---------------|------------------|
| | Estimate | Std. Error | z value | Pr(> z) |
| (Intercept) | 0.52 | 0.52 | 1.00 | 0.316 |
| LocationSOM2 | 0.32 | 0.27 | 1.19 | 0.233 |
| LocationSOM3 | -1.20 | 0.26 | -4.69 | <0.001 |
| LocationSOM4 | -3.78 | 0.26 | -14.74 | <0.001 |
| SeasonSpring | 0.03 | 0.24 | 0.12 | 0.902 |
| SeasonSummer | 0.65 | 0.26 | 2.50 | 0.013 |
| SeasonWinter | 0.07 | 0.24 | 0.28 | 0.779 |
| Length | 0.07 | 0.02 | 4.23 | <0.001 |

Appendix 21 - Logistic regression model analyzing interactive effects of sampling location and season sampled on infection prevalence of *Renicola* sp. Values given are (from left to right): model estimate; standard error, z-value, and p-value.

| glm(Renicola_sp._Bin ~ (Location+Season+Length+Location*Season),family = binomial(link = "logit"),data) | | | | |
|--|--------------|-------------|--------------|------------------|
| | Estimate | Std. Error | z value | Pr(> z) |
| (Intercept) | 1.39 | 0.65 | 2.13 | 0.033 |
| LocationSOM3 | -2.53 | 0.58 | -4.38 | <0.001 |
| LocationSOM2 | -0.90 | 0.55 | -1.63 | 0.104 |
| LocationSOM4 | -5.46 | 0.55 | -9.88 | <0.001 |
| SeasonSpring | -1.27 | 0.58 | -2.20 | 0.028 |
| SeasonWinter | -1.57 | 0.52 | -2.99 | 0.003 |
| SeasonSummer | -0.68 | 0.63 | -1.07 | 0.282 |
| Length | 0.08 | 0.02 | 4.65 | <0.001 |
| LocationSOM3:SeasonSpring | 1.28 | 0.72 | 1.78 | 0.075 |
| LocationSOM2:SeasonSpring | 1.60 | 0.83 | 1.93 | 0.054 |
| LocationSOM4:SeasonSpring | 2.06 | 0.69 | 2.99 | 0.003 |
| LocationSOM3:SeasonWinter | 2.60 | 0.82 | 3.17 | 0.002 |
| LocationSOM2:SeasonWinter | 1.83 | 0.72 | 2.53 | 0.011 |
| LocationSOM4:SeasonWinter | 2.39 | 0.66 | 3.63 | <0.001 |
| LocationSOM3:SeasonSummer | 1.61 | 0.78 | 2.07 | 0.039 |
| LocationSOM2:SeasonSummer | 1.23 | 0.86 | 1.42 | 0.155 |
| LocationSOM4:SeasonSummer | 1.95 | 0.72 | 2.73 | 0.006 |



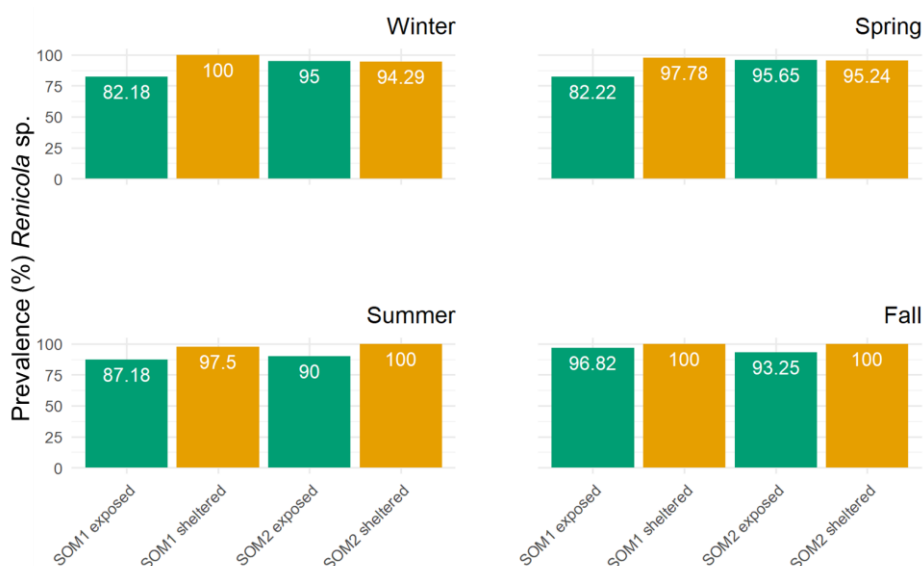
Appendix 22 - Prevalence of *Renicola* sp. at different locations throughout all seasons (SOM1 orange, SOM2 blue, SOM3 yellow, SOM4 green). Displayed in a bar chart with prevalence in percentages indicated in white.

Appendix 23 - Logistic regression model showing effects of wave exposure on prevalence of *Renicola* sp. Values given are (from left to right): model estimate; standard error, z-value, and p-value.

| glm(Renicola_sp._Bin ~ (Wave_exposure+Length),family = binomial(link = "logit"), data) | | | | |
|--|--------------|--------------|--------------|------------------|
| | Estimate | Std. Error | z value | Pr(> z) |
| (Intercept) | -0.544 | 0.719 | -0.756 | 0.450 |
| Wave_exposuresheltered | 1.45 | 0.44 | 3.32 | 0.001 |
| Length | 0.112 | 0.028 | 3.996 | <0.001 |

Appendix 24 – Logistic regression model showing interactive effects of wave exposure and sampling location as well as wave exposure and season on infection intensity of *Renicola* sp. Values given are (from left to right): model estimate; standard error, z-value, and p-value.

| glm(Renicola_sp._Bin ~ (Wave_exposure+Length+Wave_exposure*Season+Location*Wave_exposure), family = binomial(link = "logit"), data) | | | | |
|---|-------------|-------------|-------------|--------------|
| | Estimate | Std. Error | z value | Pr(> z) |
| (Intercept) | 0.310 | 0.901 | 0.344 | 0.731 |
| Wave_exposuresheltered | 16.01 | 743.51 | 0.02 | 0.983 |
| Length | 0.09 | 0.03 | 2.72 | 0.007 |
| SeasonSpring | -0.56 | 0.44 | -1.29 | 0.199 |
| SeasonSummer | -0.36 | 0.48 | -0.75 | 0.456 |
| SeasonWinter | -0.64 | 0.36 | -1.78 | 0.074 |
| LocationSOM2 | 0.30 | 0.30 | 1.01 | 0.315 |
| Wave_exposuresheltered:SeasonSpring | -14.58 | 743.51 | -0.02 | 0.984 |
| Wave_exposuresheltered:SeasonSummer | -13.35 | 743.51 | -0.02 | 0.986 |
| Wave_exposuresheltered:SeasonWinter | -14.26 | 743.51 | -0.02 | 0.985 |
| Wave_exposuresheltered:LocationSOM2 | -0.89 | 0.93 | -0.95 | 0.340 |



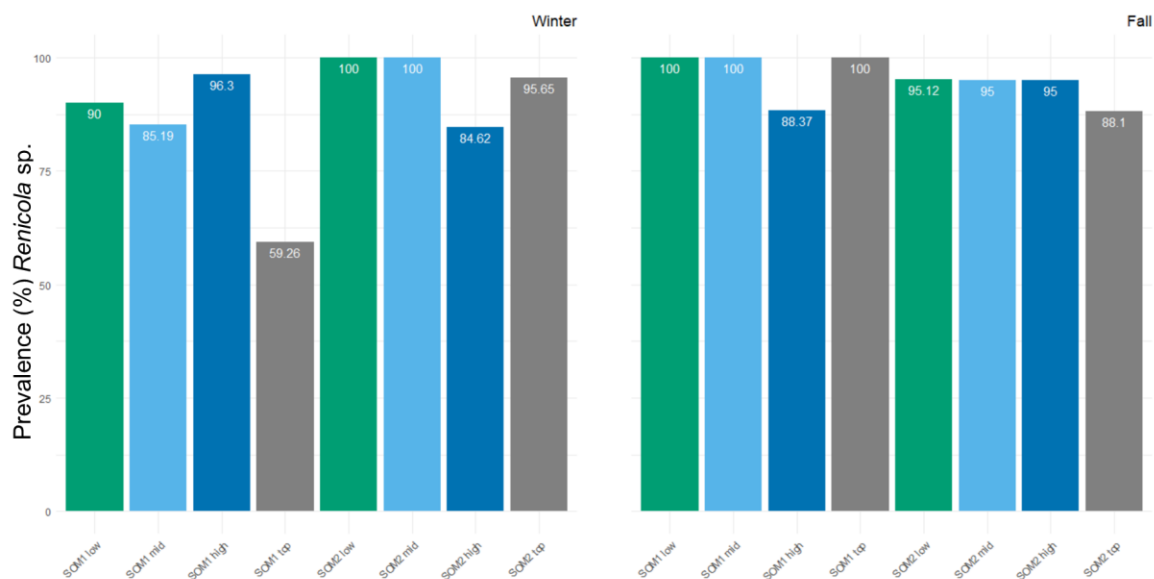
Appendix 25 - Prevalence of *Renicola* sp. at wave-exposed (green) and wave-sheltered (orange) sites throughout all seasons on a log₁₀ scale. Displayed in a bar chart with prevalence in percentages indicated in white.

Appendix 26 – Logistic regression model showing differences among the various intertidal levels, top; high; mid, and low on infection likelihood with *Renicola* sp. Values given are (from left to right): model estimate; standard error, z-value, and p-value.

| glm(formula = Renicola_sp._Bin ~(Intertidal_level+Length),family = binomial(link = "logit"), data) | | | | |
|--|-------------|-------------|-------------|--------------|
| | Estimate | Std. Error | z value | Pr(> z) |
| (Intercept) | -0.17 | 1.05 | -0.16 | 0.875 |
| Intertidal_levellow | 0.82 | 0.60 | 1.37 | 0.170 |
| Intertidal_levelmid | 0.69 | 0.52 | 1.34 | 0.181 |
| Intertidal_leveltop | -0.30 | 0.40 | -0.73 | 0.464 |
| Length | 0.09 | 0.04 | 2.42 | 0.016 |

Appendix 27 – Logistic regression model showing interactive effects of intertidal level and season as well as the intertidal level and location on infection prevalence of *Renicola* sp. Values given are (from left to right): model estimate; standard error, z-value, and p-value.

| glm(formula = Renicola_sp._Bin ~ (intertidal_level+Length+intertidal_level*Season+intertidal_level*Location), | | | | |
|---|-------------|-------------|-------------|--------------|
| | Estimate | Std. Error | z value | Pr(> z) |
| (Intercept) | 0.310 | 0.901 | 0.344 | 0.731 |
| Conditionsheltered | 16.01 | 743.51 | 0.02 | 0.983 |
| Length | 0.09 | 0.03 | 2.72 | 0.007 |
| SeasonSpring | -0.56 | 0.44 | -1.29 | 0.199 |
| SeasonSummer | -0.36 | 0.48 | -0.75 | 0.456 |
| SeasonWinter | -0.64 | 0.36 | -1.78 | 0.074 |
| SiteSOM2 | 0.30 | 0.30 | 1.01 | 0.315 |
| Conditionsheltered:SeasonSpring | -14.58 | 743.51 | -0.02 | 0.984 |
| Conditionsheltered:SeasonSummer | -13.35 | 743.51 | -0.02 | 0.986 |
| Conditionsheltered:SeasonWinter | -14.26 | 743.51 | -0.02 | 0.985 |
| Conditionsheltered:SiteSOM2 | -0.89 | 0.93 | -0.95 | 0.340 |



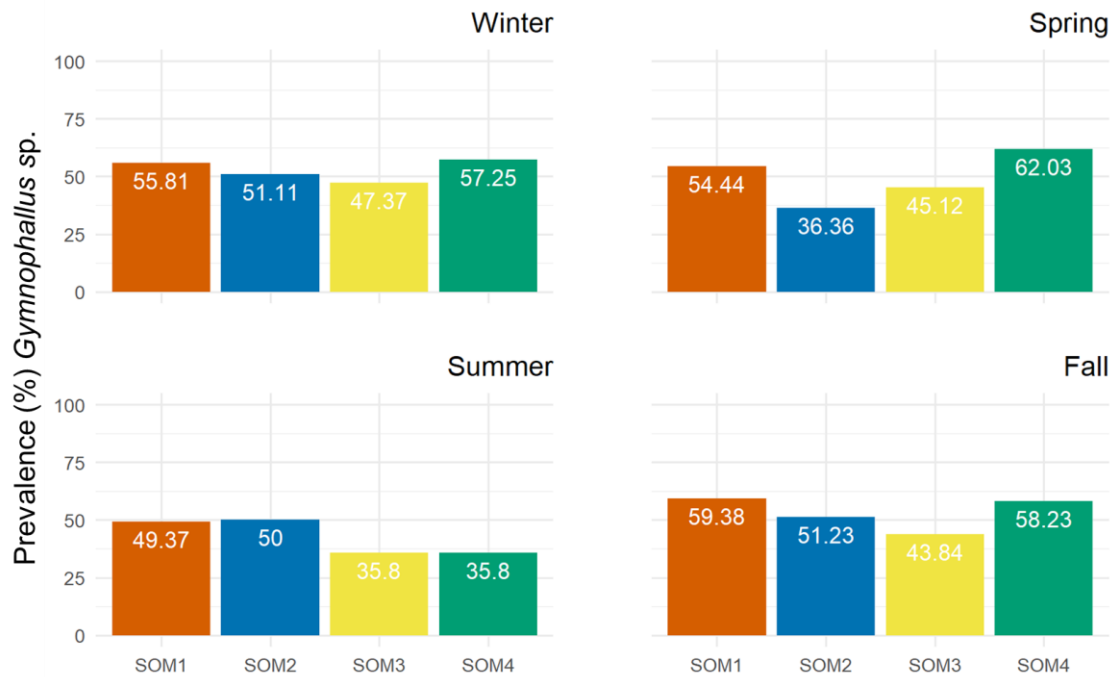
Appendix 28 - Prevalence of *Renicola* sp. at different levels along the intertidal zone ('low' green, 'mid' light blue, 'high' dark blue, 'top' grey) at locations SOM1 and SOM2 during winter and fall. Displayed in a bar chart with prevalence in percentages indicated in white.

Appendix 29 – Generalized linear model showing differences in infection likelihood with *Gymnophallus* sp. between sampling locations and seasons. Values given are (from left to right): model estimate; standard error, z-value, and p-value.

| glm(Gymnophallus_sp._Bin ~ (Location+Season+Length),family = binomial(link = "logit"),data) | | | | |
|---|--------------|-------------|--------------|--------------|
| | Estimate | Std. Error | z value | Pr(> z) |
| (Intercept) | 0.16 | 0.34 | 0.48 | 0.629 |
| SiteSOM4 | -0.11 | 0.16 | -0.66 | 0.512 |
| SiteSOM3 | -0.51 | 0.16 | -3.11 | 0.002 |
| SiteSOM2 | -0.31 | 0.13 | -2.45 | 0.014 |
| SeasonSummer | -0.39 | 0.16 | -2.37 | 0.018 |
| SeasonSpring | -0.15 | 0.15 | -1.02 | 0.308 |
| SeasonWinter | -0.03 | 0.14 | -0.18 | 0.860 |
| Length | 0.01 | 0.01 | 0.59 | 0.553 |

Appendix 30 - Logistic regression model showing interactive effects of sampling location and season sampled on infection intensity with *Gymnophallus* sp. Values given are (from left to right): model estimate; standard error, z-value, and p-value.

| glm(Gymnophallus_sp._Bin ~ (Location+Season+Length+Location*Season),family = binomial(link = "logit"),data) | | | | |
|---|--------------|-------------|--------------|--------------|
| | Estimate | Std. Error | z value | Pr(> z) |
| (Intercept) | 0.05 | 0.36 | 0.13 | 0.896 |
| LocationSOM3 | -0.72 | 0.29 | -2.46 | 0.014 |
| LocationSOM2 | -0.35 | 0.20 | -1.70 | 0.089 |
| LocationSOM4 | -0.15 | 0.29 | -0.51 | 0.610 |
| SeasonSpring | -0.18 | 0.26 | -0.70 | 0.486 |
| SeasonWinter | -0.11 | 0.23 | -0.49 | 0.623 |
| SeasonSummer | -0.34 | 0.28 | -1.22 | 0.224 |
| Length | 0.01 | 0.01 | 1.03 | 0.305 |
| LocationSOM3:SeasonSpring | 0.29 | 0.42 | 0.70 | 0.485 |
| LocationSOM2:SeasonSpring | -0.41 | 0.37 | -1.11 | 0.267 |
| LocationSOM4:SeasonSpring | 0.44 | 0.42 | 1.04 | 0.299 |
| LocationSOM3:SeasonWinter | 0.34 | 0.47 | 0.74 | 0.462 |
| LocationSOM2:SeasonWinter | 0.14 | 0.32 | 0.43 | 0.668 |
| LocationSOM4:SeasonWinter | 0.09 | 0.44 | 0.20 | 0.845 |
| LocationSOM3:SeasonSummer | 0.13 | 0.43 | 0.31 | 0.759 |
| LocationSOM2:SeasonSummer | 0.36 | 0.38 | 0.95 | 0.344 |
| LocationSOM4:SeasonSummer | -0.48 | 0.42 | -1.14 | 0.254 |



Appendix 31- Infection prevalence of *Gymnophallus* sp. at different locations throughout all seasons (SOM1 orange, SOM2 blue, SOM3 yellow, SOM4 green). Displayed in a bar chart with prevalence in percentages indicated in white.

Appendix 32 – Logistic regression model showing effects of wave exposure on infection likelihood with *Gymnophallus* sp. Values given are (from left to right): model estimate; standard error, z-value, and p-value.

| glm(Gymnophallus_sp_Bin ~ (Wave_exposure+Length+Wave_exposure*Season+Wave_exposure*Location),family = binomial(link = "logit"),data) | | | | |
|--|-------------|-------------|-------------|--------------|
| | Estimate | Std. Error | z value | Pr(> z) |
| (Intercept) | -0.60 | 0.37 | -1.61 | 0.107 |
| Wave_exposuresheltered | -0.23 | 0.14 | -1.63 | 0.102 |
| Length | 0.03 | 0.01 | 2.05 | 0.040 |

Appendix 33 - Logistic regression model showing interactive effects of wave exposure and sampling as well as wave exposure and season sampled on infection likelihood with *Renicola* sp. Values given are (from left to right): model estimate; standard error, z-value, and p-value.

| glm(Gymnophallus_sp_Bin ~ (Wave_exposure+Length+Wave_exposure*Season+Wave_exposure*Location),family = binomial(link = "logit"),data) | | | | |
|--|--------------|-------------|--------------|--------------|
| | Estimate | Std. Error | z value | Pr(> z) |
| (Intercept) | -0.47 | 0.46 | -1.03 | 0.304 |
| Wave_exposuresheltered | 0.33 | 0.31 | 1.07 | 0.285 |
| Length | 0.03 | 0.02 | 1.63 | 0.104 |
| SeasonSummer | 0.07 | 0.27 | 0.25 | 0.804 |
| SeasonSpring | -0.30 | 0.24 | -1.21 | 0.224 |
| SeasonWinter | 0.01 | 0.19 | 0.07 | 0.943 |
| LocationSOM2 | -0.10 | 0.16 | -0.63 | 0.528 |
| Wave_exposuresheltered:SeasonSummer | -0.25 | 0.42 | -0.59 | 0.555 |
| Wave_exposuresheltered:SeasonSpring | -0.09 | 0.41 | -0.23 | 0.821 |
| Wave_exposuresheltered:SeasonWinter | -0.05 | 0.40 | -0.12 | 0.904 |
| Wave_exposuresheltered:LocationSOM2 | -0.81 | 0.29 | -2.82 | 0.005 |



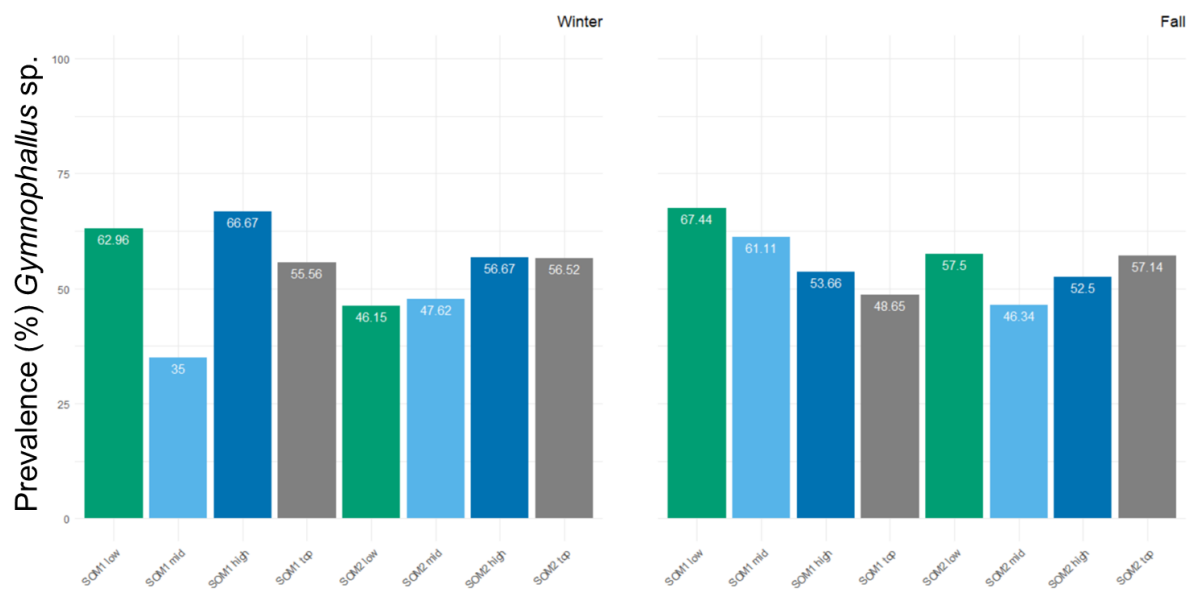
Appendix 34 - Prevalence of *Gymnophallus* sp. at wave-exposed (green) and wave-sheltered (orange) sites throughout all seasons. Displayed in a bar chart with prevalence in percentages indicated in white.

Appendix 35 - Logistic regression model showing the differences among the various intertidal levels, top; high; mid, and low on the prevalence of *Gymnophallus* sp. Values given are (from left to right): model estimate; standard error, z-value, and p-value.

| glm(formula = <i>Gymnophallus</i> _sp._Bin ~ (Intertidal_level+Length+Intertidal_level*Season+Intertidal_level*Location), family = binomial(link = "logit"), data) | | | | |
|--|--------------|-------------|--------------|--------------|
| | Estimate | Std. Error | z value | Pr(> z) |
| (Intercept) | -0.92 | 0.59 | -1.55 | 0.120 |
| Intertidal_levellow | -0.56 | 0.26 | -2.12 | 0.034 |
| Intertidal_levelmid | -0.16 | 0.25 | -0.65 | 0.516 |
| Intertidal_leveltop | -0.12 | 0.25 | -0.48 | 0.632 |
| Length | 0.05 | 0.02 | 2.31 | 0.021 |

Appendix 36 - Logistic regression model showing interactive effects of intertidal level and seasons as well as the intertidal level and location on prevalence with *Gymnophallus* sp. Values given are (from left to right): model estimate; standard error, z-value, and p-value.

| glm(formula = <i>Gymnophallus</i> _sp._Bin ~ (Intertidal_level+Length+Intertidal_level*Season+Intertidal_level*Location), family = binomial(link = "logit"), data) | | | | |
|--|--------------|-------------|--------------|--------------|
| | Estimate | Std. Error | z value | Pr(> z) |
| (Intercept) | -0.98 | 0.70 | -1.40 | 0.162 |
| Intertidal_levelmid | -0.72 | 0.41 | -1.76 | 0.079 |
| Intertidal_leveltop | -0.54 | 0.42 | -1.29 | 0.198 |
| Intertidal_levellow | -0.79 | 0.43 | -1.82 | 0.069 |
| Length | 0.06 | 0.02 | 2.74 | 0.006 |
| SeasonWinter | -0.10 | 0.37 | -0.26 | 0.794 |
| LocationSOM2 | -0.78 | 0.37 | -2.11 | 0.035 |
| Intertidal_levelmid:SeasonWinter | 0.74 | 0.51 | 1.44 | 0.149 |
| Intertidal_leveltop:SeasonWinter | 0.19 | 0.53 | 0.36 | 0.722 |
| Intertidal_levellow:SeasonWinter | -0.20 | 0.54 | -0.37 | 0.713 |
| Intertidal_levelmid:LocationSOM2 | 0.52 | 0.50 | 1.03 | 0.304 |
| Intertidal_leveltop:LocationSOM2 | 0.78 | 0.50 | 1.55 | 0.121 |
| Intertidal_levellow:LocationSOM2 | 0.51 | 0.52 | 0.98 | 0.328 |



Appendix 37 - Prevalence of *Gymnophallus* sp. at different locations with varying wave-exposures throughout all seasons ('low' green, 'mid' light blue, 'high' dark blue, 'top' grey). Displayed in a bar chart with prevalence in percentages indicated in white.

Appendix 38 – Gastropods observations at each Location (SOM1-SOM4) and site (wave-exposed and wave-sheltered) throughout all seasons (winter-fall). Gastropods were identified to species level for *Littorina obtusata* and *Nucella lapillus* while *Littorina saxatilis* and *Littorina littorea* were combined with *Littorina* spp. because of morphological similarities.

| Location | Season | Site | <i>L. obtusata</i> | <i>Littorina</i> spp. * | <i>N.lapillus</i> | Total Snails |
|----------|--------|-----------|--------------------|-------------------------|-------------------|--------------|
| SOM1 | winter | exposed | 1 | 0 | 0 | 1 |
| SOM1 | winter | exposed | 2 | 5 | 0 | 7 |
| SOM1 | winter | sheltered | 5 | 0 | 0 | 5 |
| SOM1 | winter | sheltered | 0 | 21 | 6 | 27 |
| SOM1 | spring | exposed | 1 | 1 | 0 | 2 |
| SOM1 | spring | exposed | 1 | 7 | 2 | 10 |
| SOM1 | spring | sheltered | 1 | 46 | 1 | 48 |
| SOM1 | spring | sheltered | 1 | 8 | 0 | 9 |
| SOM1 | summer | exposed | 12 | 36 | 0 | 48 |
| SOM1 | summer | exposed | 29 | 28 | 5 | 62 |
| SOM1 | summer | sheltered | 13 | 0 | 4 | 17 |
| SOM1 | summer | sheltered | 9 | 20 | 2 | 31 |
| SOM1 | fall | exposed | 3 | 4 | 0 | 7 |
| SOM1 | fall | exposed | 1 | 0 | 0 | 1 |
| SOM1 | fall | sheltered | 3 | 4 | 1 | 8 |
| SOM1 | fall | sheltered | 1 | 8 | 1 | 10 |
| SOM2 | winter | exposed | 0 | 0 | 0 | 0 |
| SOM2 | winter | exposed | 0 | 0 | 0 | 0 |
| SOM2 | winter | sheltered | 9 | 0 | 0 | 9 |
| SOM2 | winter | sheltered | 8 | 0 | 1 | 9 |
| SOM2 | spring | exposed | 0 | 0 | 0 | 0 |
| SOM2 | spring | exposed | 0 | 0 | 0 | 0 |
| SOM2 | spring | sheltered | 8 | 0 | 0 | 8 |
| SOM2 | spring | sheltered | 9 | 0 | 0 | 9 |
| SOM2 | summer | exposed | 17 | 5 | 5 | 27 |
| SOM2 | summer | exposed | 0 | 4 | 1 | 5 |
| SOM2 | summer | sheltered | 4 | 3 | 1 | 8 |
| SOM2 | summer | sheltered | 7 | 12 | 0 | 19 |
| SOM2 | fall | exposed | 9 | 0 | 0 | 9 |
| SOM2 | fall | exposed | 2 | 0 | 0 | 2 |
| SOM2 | fall | sheltered | 0 | 1 | 0 | 1 |
| SOM2 | fall | sheltered | 1 | 19 | 0 | 20 |
| SOM3 | winter | exposed | 0 | 0 | 0 | 0 |
| SOM3 | winter | exposed | 0 | 5 | 0 | 5 |
| SOM3 | winter | sheltered | 18 | 1 | 1 | 20 |
| SOM3 | winter | sheltered | 14 | 4 | 0 | 18 |
| SOM3 | spring | exposed | 0 | 20 | 0 | 20 |
| SOM3 | spring | exposed | 0 | 74 | 0 | 74 |
| SOM3 | spring | sheltered | 7 | 12 | 1 | 20 |
| SOM3 | spring | sheltered | 0 | 109 | 2 | 111 |
| SOM3 | summer | exposed | 7 | 47 | 0 | 54 |
| SOM3 | summer | exposed | 0 | 17 | 0 | 17 |
| SOM3 | summer | sheltered | 55 | 231 | 8 | 294 |

| | | | | | | |
|------|--------|-----------|----|-----|---|-----|
| SOM3 | summer | sheltered | 46 | 64 | 2 | 112 |
| SOM3 | fall | exposed | 0 | 56 | 0 | 56 |
| SOM3 | fall | exposed | 2 | 158 | 0 | 160 |
| SOM3 | fall | sheltered | 14 | 135 | 0 | 149 |
| SOM3 | fall | sheltered | 22 | 26 | 0 | 48 |
| SOM4 | winter | exposed | 8 | 7 | 0 | 15 |
| SOM4 | winter | exposed | 4 | 1 | 0 | 5 |
| SOM4 | winter | sheltered | 3 | 0 | 0 | 3 |
| SOM4 | winter | sheltered | 1 | 0 | 0 | 1 |
| SOM4 | spring | exposed | 2 | 15 | 0 | 17 |
| SOM4 | spring | exposed | 0 | 32 | 0 | 32 |
| SOM4 | spring | sheltered | 1 | 6 | 0 | 7 |
| SOM4 | spring | sheltered | 0 | 21 | 0 | 21 |
| SOM4 | summer | exposed | 6 | 39 | 0 | 45 |
| SOM4 | summer | exposed | 47 | 2 | 0 | 49 |
| SOM4 | summer | sheltered | 8 | 0 | 0 | 8 |
| SOM4 | summer | sheltered | 77 | 7 | 0 | 84 |
| SOM4 | fall | exposed | 0 | 8 | 0 | 8 |
| SOM4 | fall | exposed | 1 | 21 | 0 | 22 |
| SOM4 | fall | sheltered | 22 | 26 | 0 | 48 |
| SOM4 | fall | sheltered | 24 | 19 | 0 | 43 |

*Combined *L. saxatilis*/*L. littorea*

Appendix 39 – A) Prevalence of *Renicola* sp. from previous studies (Benito et al., 2022; Galaktionov et al., 2015) compared to the current study results. From left to right, study locations have been ordered along a latitudinal gradient (southernmost to northernmost sites). **B)** Prevalence of *Gymnophallus* sp. from previous studies (Benito et al., 2022; Galaktionov et al., 2015) compared to the current study results. From left to right, study sites have been ordered along a latitudinal gradient (southernmost to northernmost sites).

